Cape Peninsula University of Technology

AGENT-BASED ENERGY MANAGEMENT SYSTEM FOR REMOTE COMMUNITY MICROGRID

by

Arno Vosloo

thesis submitted in partial fulfilment of the
requirements for the degree:
Master of Technology: Electrical Engineering
in the
Faculty of Electrical Engineering
at the
Cape Peninsula University of Technology

Supervisor: Dr. A. K. Raji

Bellville Campus

Date submitted: 1 June 2015

DECLARATION

I, Arno Vosloo, declare that the content of this thesis represents my own unaided work, and that the thesis has not previously been submitted for academic examination towards any qualification. Furthermore, it represents my own opinions and not necessarily those of the Cape Peninsula University of Technology.

Signed **Date**

NOMENCLATURE

AC	-	alternating current
AE	-	alternative energy
Ah	-	ampere-hours
AI	-	artificial intelligence
BPL	-	band-pass limiter
CAFD	-	computer aided fixed design
CERTS	-	Consortium for electric reliability technology solution
CPU	-	central processing unit
DC	-	direct current
DER	-	distributed energy resource
EMS	-	energy management system
FIPA	-	Foundation for intelligent physical agent
HEM	-	home energy management
ILS	-	intelligent load shedder
I_m	-	maximum current
I/O	-	input / output
I_{sc}	-	short–circuit current
IT	-	information technology
MAS	-	multi-agent system
NOCT	-	nominal operating cell temperature
PCC	-	point of common coupling
PLC	-	programmable logic controller
P_{max}	-	maximum power
PV	-	photovoltaic
RE	-	renewable energy
RES	-	renewable energy source
RLC	-	resistor inductor capacitor
SANS	-	South African National Standards
SCADA	-	supervisory control and data acquisition
SMES	-	superconducting magnetic energy storage
SOC	-	state-of-charge
STS	-	static transfer switch
$V_{battery}$	-	battery voltage
V_m	-	maximum voltage
V_{oc}	-	open circuit voltage

ABSTRACT

Rural communities are often unable to access electrical energy due to their distant location away from the national grid. Renewable energy sources (RESs) make it possible to provide electrical energy to these isolated areas. Sustainable generation is possible at a local level and is not dependant on connection to a national power grid.

Microgrids are small scale, stand-alone electricity networks that harness energy at its geographical location, from natural resources. These small scale power grids are either connected to a national grid or operate separately by obtaining their power from an RES. Microgrids are becoming increasingly popular because they can provide electricity, independently of the national grid.

The size of microgrid systems are dependent on the amount of energy that needs to be drawn and the amount of energy that has to be stored. Mechanical and electrical system component sizes become bigger due to increased operational energy requirements. Increases in component sizes are required on growing power networks when higher current levels are drawn.

Energy management of microgrids must thus be introduced to prevent overloading the power grid network and to extend the operational life of the storage batteries. Energy management systems consist of different components which are seen as operational units. Operational units are responsible for measurement, communication, decision–making and power supply switching control, to manipulate the power output to meet the energy demands. Due to the increasing popularity of DC home appliances, it is important to explore the possibility of keeping these microgrids on a DC voltage basis. Electrical generation equipment such as photovoltaic panels can be used to generate DC at designed voltage levels. The energy management system connects the user loads and generation units together to form the microgrid.

The aim of this study was to carry out the design of an agent–based energy management system for rural and under-developed communities. It investigates how the control of the output of the energy management system can be carried out to service the loads. The simulations were done using the following software packages: Simulink, Matlab, and SimPowerSystems.

PV sources, energy management system (EMS) and user load parameters are varied in the simulation software to observe how the control algorithm executes load shedding. A stokvel-type charge share concept is dealt with where the state-of-charge (SOC) of batteries and user consumption will determine how grid loads are managed. Load shedding within the grid

is executed by monitoring energy flow and calculating how much energy is allowed to be used by each consumer. The energy management system is programmed to always provide the largest amount of energy to the consumer with the lowest energy consumption for each day. The batteries store surplus electrical energy during the day. Load shedding starts at 18:00 each day. Users will be disconnected from the grid whenever their allotted energy capacity were depleted.

ACKNOWLEDGEMENTS

Many thanks go to my supervisor Dr. Atanda Kamoru Raji for his technical guidance and support during the course of this research.

I thank my wife Ursula Vosloo for her continuous support and belief in me throughout this course.

I thank God for the role and discipline He has given me to complete my studies up to this point and thank Him deeply for always providing me with the drive and courage to fulfil my dreams.

TABLE OF CONTENT

LIST OF FIGURES

LIST OF TABLES

GLOSSARY

Agent	=	An agent can be a physical or simulated object that can interact, observe its surroundings in a partial way, communicate and negotiate with others, and has skills to achieve its goals and tendencies.
National grid	=	National or regional electricity distribution grid.
Scope block	=	Standard Matlab recording block to show measurements and display graphs.
Stokvel	=	A savings investment society to which members make regular payments over a specific period and then in turn, receive all or part of the money collected in that period.

1. INTRODUCTION

1.1. Statement of research problem

Communities in rural Africa are widespread and are often spread wide apart and isolated. Due to this isolation energy suppliers find it difficult to supply electricity to these regions, as both the capital and running costs for long–distance power transmission, can be quite high. Also, suppliers must provide suitably skilled personnel and deploy equipment from other areas, as rural villages do not have the required infrastructure or the skills required to install and maintain such infrastructure linking them to the national power grid. This is the reason why much of rural sub-Saharan Africa has limited or no supply of electrical energy from a national grid (Business Times, 2014).

Basic electricity needed for cooking and lighting, which are taken for granted in urban areas, are not readily available in remote rural areas. To resolve this problem a constant source of low voltage power is required. Research has up to now, only focussed on the methods to bring electrical energy to these remote dwellings, and methods to control and manage the electricity being generated and consumed from microgrids (P. Mcgroarthy, 2012). Microgrids can be a better solution for these rural communities as they can provide the villages with their own electricity supply.

Microgrids are islanded systems that harvest, manage, distribute and consume electrical energy. A limited amount of energy can be stored by batteries. Various concept designs of microgrid technologies are being studied and practically implemented all over the world.

State-of-charge (SOC) is seen as the full range of available energy that can be delivered by a battery. This range is measureable between when a battery is fully charged and when it is carries no charge. Batteries are designed to only store a certain amount of energy. The design capacity of the battery determines the limited amount of energy that can be drawn from it. The available SOC of the batteries is distributed among the loads by the application of energy management.

1.2. Background to the research problem

Over 1.2 billion people around the world do not have access to electricity, including over 550 million people in Africa and 300 million people in India (Schnitzer et al., 2014). The traditional approach to serve these communities has been to extend the national grid where it is possible.

This approach is technically and financially inefficient for remote communities due to a combination of capital scarcity, insufficient energy available, reduced grid reliability, extended building times and construction challenges to connect remote areas (Schnitzer et al., 2014).

As the national grid is not accessible to all rural communities, power harnessing equipment must be brought to the location of where electricity generation resources are available. Currently, rural communities without access to electricity, are dependent on natural resources such as wood and coal. Other processed resources like liquefied petroleum gas, paraffin and candles are used for producing light and heat for their basic energy requirements.

Schnitzer et al. (2014) recorded that technologically and operationally, microgrid distributed systems are ready to provide communities with electricity services, particularly in rural and peri-urban areas of less developed countries. Less developed countries do not have the national grid to feed power to rural settlements. Electrical energy can be generated with the latest microgrid technology at rural settlement locations.

By installing direct current (DC) microgrids, electrical energy can be harnessed from natural sources such as wind and the irradiation from the sun. In most countries today, the national grids provide 110 V or 220 V alternating current (AC) for the low voltage applications required by households.

In order to obtain an alternating current, it must either be generated directly in its AC form, or alternatively it can also be converted to DC by means of an invertor. The electronic components of inverters and rectifiers are expensive when considered for use in manipulating voltages in EMSs. When a DC grid is considered, DC generation is directly connected to the grid. Grid loads can be fed from this DC source and the need for inverting AC to DC falls away.

This study deals with generation of DC, maintaining and managing a DC microgrid for the different agents, and the elimination of the costly process of converting AC to DC. Energy management of the grid is one of the key points to observe in these microgrids in order to manage the loads and the storage units within the system.

1.3. Objectives of the research problem

It is the intent of this study to explore an energy charge sharing strategy for an islanded DC microgrid. The system will be charged by solar energy. During the day the grid will supply electrical energy to grid users. A function inside the software must be designed to simulate changes in the irradiance level of the sun. The irradiance adjustment can be used to simulate

clouds and natural events that will diminish irradiance levels as the weather changes and also to simulate night-time, when there is no sun.

To record and store all the load user consumption figures and allow the system respond to selected prescribed load shedding algorithms, function block logic must be designed on the Matlab platform. It is envisaged power measurement points will be installed on the bus system in order to provide load management points.

To determine when load switching will take place, sensing and control units act on command signals to and from the energy management system (EMS). The system will add all the charge measurements received by the generation units. As load is applied to the respective load-points, the system will detect this load value, subtract it from the total charge load value and decide when each user will be disconnected from the system. Photovoltaic panels are used to generate electrical energy. The battery bank stores surplus electrical energy.

The energy management system will consist of measurement components and control components that will act and execute functions as agents. The control philosophy will revolve around the agents to operate the charge share control objectives. Agents form part of the system and work hand in hand to combine the overall system components. Environmental inputs, system control and execution of the software model environment will determine microgrid load shedding.

The physical location of the control agents should be determined by the system design. The power sizing per house unit per day needs to be estimated in order to obtain the total system power demand and the required system capacity. The system capacity needs to be calculated to determine the size of the batteries that will be included in the software model.

The software model should be accessible to change any parameter within the microgrid. It is vital to prepare a working platform of the microgrid on Simulink in order to support future research developments. The software model should be flexible to allow user inputs to change the dynamics and control within the microgrid and to allow the grid to react to these adjusted parameters.

1.4. Research design and methodology

The following points, as well as the methods that were used to conduct the research, were addressed during the design phase of the project:

- The methodology used in this study is quantitative. Parameter input data is processed by the simulation model.
- Software simulations are carried out to determine optimum system parameters. A simulated model of a DC microgrid was constructed using computer software. Parameters of the model were changed to create different scenarios within the grid.
- Matlab, Simulink and SimPowerSystems software programming blocks are used to construct the microgrid environment. Programming blocks are combined to form the microgrid.
- Mathematical calculations illustrated variable results of equipment functionality.
- Concept designs of microgrid layouts were considered as well as the positioning of the photovoltaic panels.
- Software parameters needed to be established to decide how load shedding is executed.

As part of the study, the following issues were addressed:

- The derivation of a mathematical formula to manage energy allocation among several user loads.
- A state-of-charge / battery model.
- The development of a bus voltage regulation technique.
- The development of a PV model to simulate differing irradiance inputs.
- The definition of load sizes.
- The generation of load blocks.
- The definition of switching control parameters.
- Investigation of time functions for day-night simulation.

- Identification of battery charge/discharge control parameters.

- Comparison of normal discharge loads to manage discharge loads.

Due to the nature of this study, most of the emphasis was placed on the design of the model using MATLAB tool. The model was divided into subsystems; these subsystems are connected to each other to form signal circuits and physical circuits. Load shedding of the loads is controlled by monitoring power consumption.

1.5. Research questions

The following questions were formulated before the research project was started:

- How can microgrids in rural communities be made more efficient by the energy management control algorithms?
- In order to accomplish a charge share concept, how will the definition of the software model determine the control algorithm?
- How is load shedding determined and to which parameters will it respond?
- Looking at the power consumption for each house unit, how will the SOC fluctuate during load shedding and during the charging phase of the day?
- By introducing the reserve share management algorithm, will the system be able to be used for a longer time by each user under specific load conditions?
- Will all the users benefit from the power share design?

1.6. Significance of the research

The following contributions can be attributed to the outcome of this research:

- A reduction in the cost of hardware, by using a DC voltage microgrid; this eliminates the need for AC inversion techniques and components as required in conventional AC microgrids.

- Providing communities and authorities with the option of a source of electricity, independent of the national grid.

- Feeding electricity directly into the microgrid from the DC bus, in a controlled manner by the energy management system.

- A conceptual software design to control a limited low-voltage, DC power supply for rural communities; control is via an agent-based management system.

- To introduce an electrical charge share concept tested on Simulink, Matlab, and SimPowerSystems.

- A simulated test bed, available for future development and testing of the modelled microgrid environments.

- A charge system that calculates and controls load shedding, based on the stokvel concept, where consumer privileges are calculated and available energy is distributed according to daily consumption.

- The concept design developed, can serve as the basis for the distribution of power in microgrid EMSs.

- Not only can this control scheme be used for rural communities, but it can also be used in power distribution for various commercial and residential applications.

- This concept was not tested in a laboratory test bed environment or carried out with hardware testing. Simulation software test bed was developed and results were obtained from the simulation model.

1.7. Expected outcomes, results and contribution of the research

Expected outcomes from this research are a defined control algorithm to manage the energy storage and load power consumption in a microgrid. The control of energy consumption is effected through load shedding. The microgrid will have control over all the switching devices and will control them according to battery charge level and system parameters.

This research is expected to produce the following results:

- Data logging of user power consumption by users.

- The design of the power distribution network within a microgrid.

- To use a software simulation package to simulate the bus system, control units and the control parameters of a microgrid.

- In accordance with the stokvel concept, active users will enjoy longer operation times at a particular time of the day when other users are not connected to the grid or not consuming power. The remaining energy in the battery bank of the microgrid will be divided between users at sunset.

- A reserve share formula will be derived which will allow energy to be divided from the remaining battery SOC among all the users.

1.8. Organisation of the thesis

The thesis starts with the introduction in Chapter 1. Background information to the research is discussed and is further explained by the objectives to be achieved. Methods on how the research is conducted, are explained. Matlab is used to build the software simulation platform and a list of research questions has been formulated to serve as the basis for the goals to be achieved. The expected outcomes section gives a list of items of expected results to be achieved. These results give information to drive future projects based on this work. Finally the chapter concludes with a description of the organisational structure of the whole thesis, providing a quick-glance summary of the thesis content.

Chapter 2 deals with the literature review at the start of this research project. Generation methods in general are discussed to give a broad overview of existing methods of alternative energy. Energy management systems are introduced and different control designs within the industry are described, as well as how future development could change these technologies.

Chapter 3 introduces agent-based technologies. Communication procedures and agent coordination are brought together to deal with the modes of grid operation. A few microgrid examples show the remoteness of their geographical locations and the implementation of energy management around the world.

Chapter 4 describes an example on how the selection of solar panels and batteries is done for a microgrid. Calculations to determine the required number of solar panels to harvest energy for a the microgrid; this gives the reader an idea of which parameters are required to design the generation and battery storage units for a multi-agent system (MAS) network.

A detailed explanation, indicating the functionality of Matlab design software, is given in Chapter 5. A general overview presents information on how the program fits together. Subsystems are subsequently broken down into logic blocks. Technical aspects within the program are discussed. The charge share formula is taken apart to show how the share charge values are derived. Further content deals with the multi-agent system design. Within the Matlab model, each functional block and subsystem is taken apart and explained in detail. The control functions and the reason for their use are explained.

Chapter 6 gives the Matlab model user a guide towards setting up the model prior to simulation runs. Further into the chapter, four scenarios are set up and each one is produced in a tabular form.

In Chapter 7 the results of each scenario, as described in Chapter 6, is presented. The results are presented graphically and are summarised in a table at the end of each section dealing with the particular test. The electrical charge share formula was derived using Excel and coordinates were compared to the results from the corresponding simulation run.

Chapter 8 gives the project results and conclusions. Recommendations for future research work are presented. These ideas can be used to expand the work of this thesis, into more complex simulation models.

And finally, after Chapter 8, there is provided a list of references.

2. LITERATURE REVIEW

2.1. Microgrid layout

Figure 2.1 shows a 13.5 kW photovoltaic system in Makueni County in Kenya (Phys. Org, 2013). This generation unit was designed and build to provide water and electricity for the local community. Note that the DC generating PV array shown in Figure 2.1, is centrally located in the village. Solar panels are used to convert solar energy into electrical energy. Microgrids seldom have long transmission lines to supply power to other towns and areas far from the point of generation.

Figure 2.1: Makueni County 13.5 kW PV system, Kenya, Kitonyoni village market (Phys. Org, 2013)

The extent of the distribution network is determined by the location of the generation equipment and storage units, relative to the location of the loads. Energy management is applied to control the use of the limited output available from the power generation unit.

2.2. Generation methods AC versus DC

In the 'War of Currents' era in the late 1880s, George Westinghouse and Nikola Tesla (recognized for AC inventions) and Thomas Edison (inventor of DC generation) became opponents due to Edison's promotion of DC for electric power distribution over AC (Lantero, 2013). DC and AC technologies were compared during the late 1880s. AC and DC generator technologies have since evolved to the methods of power generation and motor technologies of today. AC technology was favoured by early users due to the ease of stepping voltages up or down, by using transformers.

In 1839 inventor Endmond Bequerel created the world's first photovoltaic cell (Zamostny, 2013). From that time, photovoltaic technology has evolved to become one of the most attractive renewable electricity generation technologies in the world. It is an independent technology that generates DC.

Photovoltaic cells are connected in series and parallel to form a cluster of cells. These clusters together are known as a solar panel. Solar arrays are formed by joining solar panels into series and parallel configurations. Solar arrays used in microgrid networks nowadays and are found in many off grid systems.

Alternative energy systems have different ways to convert natural energy into electrical energy. These systems have a low level of contamination on the environment. Energy generated by solar panels is directly obtainable from nature and does not require multiple energy conversions to arrive at electricity form.

2.3. Limitations in area of use

A shortcoming of solar systems is that the energy source is dependant on the prevailing weather. In overcast conditions, the irradiation levels are lower. If no wind is present then wind generation is not possible. These two sources are widely used in conjunction with each other to form hybrid systems.

Palma-Behnke et al. (2012) stated that one of the biggest challenges in microgrid development is local capacity building. These energy projects are generally more successful where villagers engage actively with the process from the construction to the operational phase. Communities have to understand that energy provision is more than just a service and that they need to participate in the process of managing and maintaining such energy systems. People also have to communicate with one another to ensure that they benefit from an energy system, as they have to share their limited communal energy capacity throughout the day and night. Energy management systems are capable of allocating and adjusting the supply to meet the needs of the microgrid consumer, within limits.

Variation in irradiation energy obtained from the sun requires different harnessing methods to absorb natural energy. Charge controllers produce high efficiency charging of the batteries. Solar panels provide their current and voltage signal to the charge controller. The voltage and current are converted to accommodate efficient battery charging. PV systems benefit greatly from charge controller technologies. Designs and methods are widely studied and tested to achieve optimal performance from hybrid systems.

The battery SOC level determines the duration of use of electrical energy at night when the microgrid is operational. Battery condition, charge and load management, are critical to sustain the storage capacity. The battery charge capacity is also a major limitation to be considered. If the battery charge level becomes too low during the night, the grid is likely to shut down completely.

2.4. Generation technologies / Energy storage

Generation methods and energy storage methods are explained by Nehrir et al. (2011) and are summarised in Table 2.1. Proper optimization techniques and control strategies are needed for sizing in microgrids (Nehrir et al., 2011). System performance can be enhanced when a combination of renewable energy (RE) resources and alternative energy (AE) resources are used.

Table 2.1: RE/AE generation technologies and energy storage types (Nehrir, 2011)

Main RE/AE Technology
Biomass
Geothermal
Hydro/micro hydro
Ocean tidal / wave
Wind
Fuel cell
Micro turbine
Solar PVs/thermal

Energy Storage Type
Battery
Compressed air
Flywheel
Hydrogen
Pumped hydro
Superconducting magnetic energy storage
Thermal
Super capacitors

2.5. Distribution

Syed (2012) states that “with the increasing penetration of renewable power sources and impending increase in the number of appliances that run on DC power, it makes a lot sense to develop DC microgrid and DC supply systems, especially in rural areas." Research on DC appliances should be encouraged, to make the use of a DC standard more viable.

Investigations have previously been done on voltage level standards for DC home microgrids (Li et al., 2012). Voltage levels and wire cross-section sizes for different load groups are very important factors to consider in microgrid designs. These parameters do determine how much power can be transported throughout the grid.

According to conductor line thermal limits, power losses, and voltage drops, previous research results show that if 120 V DC was considered for the DC bus, a higher voltage potential above 120 V will not result in further efficiencies in the transmission of the power to the loads. These results were established before it was found that, due to high losses, 24 V DC could only be used for extra-low power appliances in a small house or a single room. Instead, 48 V DC may be better suited to lighting and low-power appliances; according to Li et al. (2012) it is likely that 48 V DC will be the standard for this type of application in the future.

The South African national standard on the wiring of premises (SANS 10142-1: 2009) only make reference to voltage levels up to 50 V DC. Microgrids are still being constructed under many different grid configurations and are being investigated. It is therefore still an open platform to choose the voltage level at which a microgrid will operate; the choice often depends on the ratings of the generation units and converters available. It is considered to be a safer voltage to have a bus system below 50 V DC.

2.6. Energy management systems and methods

Testing of energy management systems in established microgrids is very limited because of the low number of such installations, however Radziszewska & Nahorski (2013) has found that testing can be done with software-simulated models, using direct measurements collected from a few devices. Configurations in different geographical locations are not the same due to huge differences in culture, climate and wealth of different regions. These differences determine how software simulators are set up.

The EMSs of microgrids contain hardware and software protocols to form the operational platform of these control systems. Control and monitoring is moving towards the use of an automated agent technology using a multi-agent system (Manickavasagam et al., 2011).

Multi-agent systems take intelligent decisions on behalf of the user, instead of the more traditional supervisory control and data acquisition (SCADA), which is not as flexible and requires regular monitoring and human intervention (Manickavasagam et al., 2011).

Load scheduling of MASs was presented in research done by Logenthiran et al. (2010). Load scheduling is a way to optimize microgrid operation efficiency by looking at load recordings and paying particular attention to reducing the peak sections. By reducing peak load consumption during the day, it can result in extended energy use during the night, as the surplus energy available when peak usage is reduced, and thus be stored.

For microgrid layouts, there are different ways of integrating renewable resources with the community. In a paper by Potty (2013) it is stated that various control methods are achieved by using different control components in the smart grid environment. Smart meters and smart stations form two essential parts whereby communication techniques share data in control architecture. Smart meters capture user power consumption and these figures are communicated to smart stations. Smart stations are linked to the aforementioned control architectures.

Jian (2014) presented a multi agent-based control framework where new types of power supplying modes that have a promising future in the design of such frameworks. His research showed a software model that was broken down into three layers of operation; these layers include main grid agents, microgrid agents and component level agents. Coordination control represents more efficient load control and charging due to the effective communication database between the three layers of operation.

Li et al. (2012) states that these grids are attracting considerable attention owing to the increasing prevalence of DC home appliances and distributed energy resources. This study motivates for the 48 V DC bus to be considered as the grid bus voltage level of choice.

Chaouachi et al. (2013) explained that artificial intelligence techniques in cooperation with linear-programming-based, multi-objective optimization systems are being tested. Energy management in these systems aim to minimize the operational cost and the environmental impact of a microgrid. In order to manage future loads, these systems also take into account the load demands of operational variables.

In a different study by Chaouachi et al. (2013), they claimed that results from their control methods are also useful to extend battery charge and discharge cycles on a scheduled basis. These methods were obtained by using software models and weather forecasting data. The results were used to compare actual and predicted weather profiles several days ahead. These systems can hereby determine how load shedding can be controlled in the

days to come. Efficiency of these microgrid operations is strongly dependent on the battery scheduling process, which in turn is influenced by software systems which are programmed to anticipate weather conditions. Stluka et al. (2011) stated that forecasting will mostly be based on a short-term forecasting concept. Stable cloud patterns lead to better predications of future weather patterns, whereas unstable cloud formations make such predictions more difficult. Taking account of the predicted weather conditions, the system will consider the current state-of-charge of the storage units and determine the corresponding amount of energy that it will have to allocate for consumption. The system will cut back the distribution allowance to the loads and conserve energy if it is determined that little charging opportunity may occur in the coming days; this facilitates extending the energy storage buffer of the system.

A different load-scheduled control strategy is explored by Michaelson et al. (2013). Predicted generation is combined with predicted load. Past load patterns are available from load recordings made at the specific site. Automated load shedding can be scheduled when the system can calculate during which future period the grid will be under severe strain. Such a situation will occur due to overloading or the unavailability of energy if the SOC of the batteries is too low. Future prediction of the SOC trajectory is achieved by this power management strategy.

Polycarpou (2013) supports the idea that smart grids enable consumers to decide when they want to use power from the grid. Strictly speaking it is said that microgrid philosophy is not a new concept, as it has been in use for as long as electricity grids have been inexistence. The control philosophy is new and this is where emphasis on study should be. Modern control systems have resulted in smart microgrids, to the point where these grids can easily shift loads, based on differing needs and desired outcomes.

As described by Ramesh et al. (2013), Arduino-controller-based systems have been incorporated in actual microgrid installations; this type of system is described as a MAS. Arduino is a microcontroller that is programmed by open source software, to fit the needs of any programmer. Furthermore, many other types of microcontrollers are used to perform monitoring and control of microgrid systems. To build a central control system, external power modules are inserted into the I/O slots. The unit acts as a programmable logic controller (PLC) and can be expanded to control and manage systems accordingly.

Palma-Behnke et al. (2012) explained that smart grids are characterized by a two-way flow of electricity and information. These smart grids are capable of monitoring everything from power plants to customer preferences, as well as individual appliances. Real-time deliverable information is acquired and enables the near-instantaneous balance of supply and demand

at device level. Real-time information can operate at different intervals as long as it is located near the source of energy and near the areas of supply delivery.

The three different levels into which the energy management system of a microgrid can be divided, are explained by Meiqin et al. (2011). These areas form a pyramid structure with linking layers between them. The top layer forms the local control level. Within this level communication agents, control agents and the status agent are present. The SCADA platform is found at the centre level. All the server agents and recording facilities are connected to the SCADA system. Level three is the system control level. Control of the system is exercised at this level via the system operator agents. Grid status and switching between islanded mode and grid-connected mode is set here.

Boynuegri et al. (2013) defined a load-shifting algorithm for home energy management (HEM) whereby the centre of control is dependant on the SOC of the batteries. By introducing these peak-shaving and load-shifting techniques, a saving of 25% was evident from these simulation results. A study of battery capacity was done to compare battery sizing when batteries are put variously under charge, and discharge conditions. From this battery system, energy was also sold to the main grid. Microgrid battery systems should not be oversized or undersized. Oversized battery systems do not get sufficient consumption drainage and undersized systems will be depleted very quickly depending on the amount of energy drawn from the battery system. From an evaluation done by Yen-Haw et al. (2011), it was shown that systems should be sized by battery efficiency and the power supply generators.

Intelligent load management functions were studied by Kennedy et al. (2012). Their focus on this topic was to approach load management through a load shedding scheme. They proposed an intelligent load shedder (ILS) principle and works together with a static transfer switch (STS). The STS operates as the PCC between the grid supply and the user loads. Loads are systematically removed from the grid to allow the grid sources to carry the remainder of loads.

According to Hajimohamadi and Bevrani (2013), proper system controllers in the primary, secondary and emergency levels of microgrids ensure stable operation during load shedding. These controllers prevent the system from breaking down to the level of a complete blackout; they assist in shedding load in a controlled manner. Very similar to conventional systems, isolated microgrids also suffer from different events such as tripping generators, imbalance between generation and consumption, and power quality issues. All loads are not simultaneously disconnected; non-critical loads are disconnected first and then the software program will prepare for load shedding of power consumers.

From the studies above and taking account of all the cited references, it is evident that the focus is on load control techniques and battery charge methods. These systems are linked together through various communication protocol methods that act as the nerve structure of the system. Due to the limited charge capacity that is available from the batteries at sunset, focus can be directed towards load shedding control techniques around the SOC values of the batteries.

The conclusions from the above-mentioned studies serve as a motivation to incorporate a stokvel philosophy in the load control so as to develop a reserve share concept.

3. MICROGRID TECHNOLOGY

3.1. Agent-based technology

Agents are responsible for information flow within the system. The term 'agent' is characterized by the meaning of autonomy. Chang and Jai (2009) identified Agent technology consisting of networks within a microgrid systems of multi–agent modules or components which together form MASs. These networks of agents are used in the control of wind turbines and solar arrays. In addition they are responsible for directing communication in the decision-making processes, and executing actions.

Artificial intelligence (AI) is a research topic; MAS forms a subsection of distributed AI. The goal of a MAS is to disassemble a big complicated system that consists of software or hardware, into multiple in interaction and subsystems which can be easily managed. Gradually, microgrids are providing a new method for developed countries to solve problems relating to the national grid. With the intensification of the global energy crisis, the microgrid will become an important development in this sector.

The United States first proposed the concept of a microgrid. In 2002 the Consortium for Electric Reliability Technology Solutions (CERTS) stepped forward to define the concept and structure of such a system (Qin et al., 2010).

The major focus of a CERTS microgrid is to power electronic devices possessing intelligence and flexibility as their main features (Qin et al., 2010). A CERTS microgrid does not have a central master controller and works in a peer-to-peer fashion (Hernandez et al., 2013). The microgrid EMS is a fully computer-based, scheduling system and a control-based system, using advanced information technology (IT). EMSs allow for plug-and-play options to expand and change the design layouts as required.

Qin et al. (2010) explained that the idea of multi-agent systems is to divide large systems into a number of small, autonomous communication systems. Intelligent distribution system management forms the centre of these systems. A typical architecture has a central controller containing the centralized functions, and several local controllers in which local functions specific to each device, reside.

Hernandez et al. (2013) gives more details on a MASs that were developed on the Java Agent DEvelopment (JADE) framework which complies with specifications of the Foundation for Intelligent Physical Agents (FIPA). Jimeno et al. (2010) explained that according to the topology of a microgrid, control intelligence can be distributed across different controllers which will improve robustness and the required distribution of hardware resources. The

microgrid can potentially be a very dynamic system, where devices from different technologies and vendors can coexist and where they can be connected and disconnected seamlessly. By sharing the same communications framework, all these separate vendor devices will have the interconnectivity to manage one multi-agent system through plug-and-play techniques.

3.2. Microgrid communications

As microgrids expand, measurement points become more de-centralized. Increased difficulty to capture data over a larger distance has resulted in more reliance being placed on communication protocols to assist with this problem. Advanced communications technologies such as optical internet protocol (IP) networks, band-pass limiter (BPL) carrier, and broadband wireless network technology are used (Qin et al., 2010). It is very important to have as many measurement points as possible in order for the microgrid to provide flexibility in the supply of high quality. The uploading speed of data from monitoring should as fast as possible, in order to react to issues and to allow real-time control between the microgrid and its energy sources. It was pointed out by Hernandez et al. (2013) that the smart distribution network requires periodic fast measurements and estimations of network security as well as real-time information from network components.

Xinhua et al. (2007) presented three categories of communication namely: knowledge interchange format, knowledge query and manipulation language, and FIPA agent communication language. FIPA is a body for developing and setting computer software standards. In recent years the extensible mark-up language (XML) has become an acceptable language for agent communication (Xinhua et al., 2007). XML is a language used to describe a language. Different classes of documents can be defined and translated from custom languages by using XML.

Multi-agent architectures are divided into two coordination categories: centralized multi-agent coordination and de-centralized coordination.

3.3. Centralized multi-agent coordination

Figure 3.1 illustrates that coordinators are situated at the head of the architecture. They carry responsibility for communication between other agents. Within the architecture the main representatives of agent coordinators are the mediator and the facilitator. The mediator agent makes decisions on lower level situations. It is involved with message interpretation and task decomposition. A program that handles coordination between communication agents is

called the facilitator. Based on their content, routing of messages is controlled from the here, as well as regulating control of multi-agent activities.

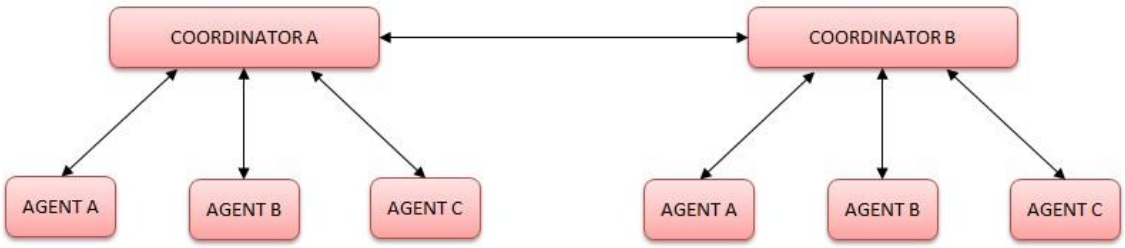

Figure 3.1: Centralized multi-agent coordination (Andreadis et al., 2014)

3.4. De-centralized multi-agent coordination

Figure 3.2 shows the de-decentralized coordination as an agent works in conjunction with linked agents; this type of coordination can be defined as autonomous. An agent operating in a de-centralized coordination setup is not controlled by software or a person; it communicates directly with the other agents in the system by always scanning the status and tasks the other agents are performing and executes its own tasks by associated motives. Communication is present between all the agents as shown in Figure 3.2 Communications to other networks are also possible by these agents.

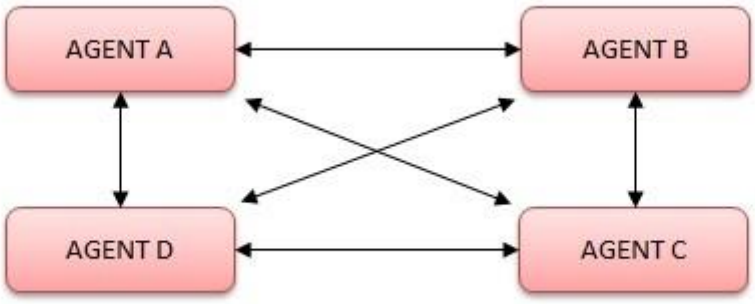

Figure 3.2: De-centralized multi-agent coordination (Andreadis et al., 2014)

3.5. Control methods

Considering continuity of supply to islanded microgrid loads and national grid loads, it is important that the power to loads is not interrupted during transitioning of the microgrid onto, or off the national grid. Developing new interface technology is constantly undertaken to handle transitions between these modes. Currently, there are three typical control methods

as explained by Qin et al. (2010), namely plug-and-play technologies, power electronic devices and control-based multi-agent technology. All three methods have progressed technologically to differing degrees, and it is understood that they will mature and grow with the application sustained development in this field (Qin et al., 2010).

3.6. Modes of operation

Microgrids can function either in isolation or together with the national grid in grid-connected mode. When operating in grid-connected mode, the microgrid will have direct coupling to the national grid. Jimeno et al. (2010) refers to this connection as the point of common coupling (PCC). A microgrid in islanded mode works in a disconnected state from the national grid. This ability allows a microgrid to be disconnected when power quality supplied by the main grid is not satisfactorily.

The focus of this study is more on islanded microgrids for rural areas not always to be close to national grids, and where a PCC is possible. In islanded mode the grid should meet the required load balance by adjusting the power supplies to in accordance with the loads. In islanded mode it is desirable to effect load shedding before the batteries get depleted.

The producer agent, storage agent and observer agent were highlighted in the study by Hernandez et al. (2013). The microgrid uses PV arrays as its source and the producer agent is responsible to communicate the nominal battery capacity to the storage agent. The storage agent monitors the storage capacity of each microgrid system. The observer agent monitors the whole system in both the simulated scenario and the measured scenario. The storage agent gives the observer agent feedback on the battery charge condition. This is a control cycle with continuous communication between the different agents.

3.7. Multi-agent modelling and implementation

In order to build a complex agent system in a simplified manner, open-source platforms are used by developers. The intention of the research by Hernandez et al. (2013) was to use the JADE Platform.

JADE facilitates the development of multi-agent peer-to-peer applications. Parameters of this system aim at the optimal use of locally distributed resources, feeding of local loads and operational simplicity. Direct support of plug-and-play can be used by the JADE-based platform.

Jimeno et al. (2010) referred to a demand profile of the grid. This is the map and baseline prediction load graph that is used for the load reference. The profile indicates the power

demand (in kW) versus time of the day. In coupled microgrids, it is vital to use this baseline as a reference when energy transfer and power flow is to be controlled. The demand profile was used as a reference to control how and when the grid sources should be adjusted to the load. Costs to run the individual source units were also monitored as load demands changed. The system makes decisions around cost and executes accordingly in order to use the most affordable option to generate energy; the system makes adjustments where needed.

3.8. Agents in the energy management systems

Schedule trackers are used to allocate set points to distributed energy resource (DER) gateways. Schedules are calculated by observing recorded data. The microgrid operator agent is used to optimize the operation of the microgrid by taking into account the information provided by the agents in the local controllers. DER operator agents are used to provide information to the microgrid level operator and also to act accordingly when receiving signals from it.

3.9. Microgrids around the world

The following examples of actual microgrid installations in rural areas, have been implemented, tested and are currently in operation. These systems are large or small scale microgrids, depending on the load demand and application.

3.9.1. Kenya

The Kitonyoni village market solar project was established in 2012 in Makueni County, Kenya. The project, shown in Figure 2.1, successfully replaced the use of candles and kerosene previously used for lighting within community households and businesses. This rural microgrid is operating on a 13.5 kW photovoltaic system (Phys.Org, 2013). The community received this generation unit to provide water and electricity for basic lighting and power to serve the community. This project is now seen as an aspirational example in Africa, and has received many local and international visitors including from Japan, Germany, the UK, Zambia, the World Bank and other funding agencies.

3.9.2. India

After many years of neglect and no assistance from local authorities, a small Indian village in the north-eastern part of India have met their own energy requirements since the beginning of 2014 (Fitzpatrick, 2014). One of the poorest regions in Bihar houses the small village of Dharnai with a population of 2400. Figure 3.3 shows the village of Dharnai which is now

served by a 100 kW system that supplies electricity to 450 homes, 50 commercial operations, and a training and health care facility. Electric energy is always available from deep cycle storage batteries. This is the first village in India which obtains 100% of its electricity from solar power.

Of the 100 kW PV system capacity, 70 kW is fed into the microgrid for general use and 30 kW is reserved. (Greenpeace, 2014).

Figure 3.3: Dharnai village in the state of Bihar, India (Fitzpatrick, 2014)

Educational opportunities have been improved by reliable electricity. The local economy has also been boosted by dependable power and brought a welcome improvement in the social life in the village.

The poor population in India uses firewood and cow dung for fire to do cooking and to use as a source of light. It does not only have a negative impact on health, but also impedes economic growth within the country. On Sunday 20 July 2014, Greenpeace commissioned the official operation of the microgrid. Greenpeace is private global campaigning organization that manages funding, construction and commissioning of environmental projects as well as microgrid projects (Greenpeace, 2014).

3.9.3. Tokelau Islands

Tokelau has a population of about 1500 people and is an island nation in the south Pacific on the eastern side of Australia. Initially the entire island was powered by three diesel generators that used a total of 200 litres of fuel per day. A solar microgrid was constructed as shown in Figure 3.4 and by October 2012 residents accomplished their goal by becoming the

first island nation in the world to produce 100% of its electricity from the sun (Chan, 2012). A 1 MW solar-PV microgrid, consisting of 4032 solar panels, 392 inverters, and 1344 batteries was constructed(Chan, 2012).

Figure 3.4: Solar panel array on Tokelau Island (Power Smart, 2012)

3.9.4. Malaysia

Bullis (2012) indicates that a 430 kW array of solar panels as shown in Figure 3.5, was installed in 2012 by Optimal Power Systems in eastern Malaysia. This system has an inverter of 250 kW to convert DC to AC which is fed into the village grid. The motivation for this project was to eliminate diesel generators and to bring clean electrical power to remote communities. It was noted that for the large scale PV array installations, the cost per kWh was cheaper than could be provided by diesel generators.

Figure 3.5: A 430 kW solar array in eastern Malaysia (Bullis, 2012)

4. SYSTEM DESIGN FOR RURAL SETTLEMENT

4.1. Introduction

The design of a three-house islanded microgrid as used in this study to serve as an example of the charge share concept. When small microgrid systems have been successfully designed, a multiplication factor can be applied to allow for an increase in the number of houses and the corresponding increase in total load that would be required for such a macro consumer design. Solar irradiance profiles for the Western Cape, South Africa, are dealt with (GeoSun Africa, 2015).

Software development packages such as Matlab are available into which the grid design parameters can be inserted. These design packages then calculate the number of solar panels to be used, the size of each unit, and determine the battery size. The designer can also enter weather and day-time parameters to monitor the microgrid as a whole.

4.2. User load demand

The case-study example below provides the times and load averages that was used to determine the system generation units. At the outset the size (kW) and duration (h) of the load demand that will consume energy from the system, needs to be established before the system generation units can be designed.

> Example: A rural house is assumed to have an average load of 1 kW. In the morning allow 3 hours consumption between 05:00–08:00. Over lunchtime two hours load are consumed between 12:00–14:00. At night 5 hours load consumption is allowed for between 18:00–23:00.

4.3. Battery sizing

To determine the battery size for a house unit, a few design specifications need to be confirmed before calculations are done. Daily energy demand needs to be considered. It must be determined for how long the loads need to be supplied per day and for how many days the system must be able to provide energy to the loads; this is known as the autonomy of the system. Following on from the example above an average power consumption of 1 kW sustained for 10 hours, yields an average daily energy requirement of 10 kWh.

The average daily energy requirement must be multiplied by a factor of 1.2–1.5 to allow for power losses due to increases in temperature and spike loads (Solar direct, 2015). This factor also allows for decreasing performance when the temperature increases. Multiplying

the required 10 kWh by the 1.5 loss factor, will give a required total battery energy rating of 15 kWh for one day.

4.4. Autonomy of the system

It must also be decided how many days' worth of energy must be stored in the battery bank. Generally, system designs allow for an autonomy range of two to five days. In the case of the example, an autonomy capacity of two days will be taken into account. The total battery energy of 15 kWh is multiplied by two and results in 30 kWh, which then gives a system autonomy of 2 days.

4.5. Battery bank capacity

Lastly the minimum battery capacity (in ampere-hours) must be calculated. To prevent a SOC below 50% for the batteries, the total battery energy should be double the required energy rating inclusive of the loss factor and the system autonomy. By multiplying the 30 kWh by two to give 60 kWh, the total battery energy capacity requirements was determined.

The capacity rating of a battery was determined by dividing its energy output by the battery voltage. A voltage of 48 V DC was chosen for the microgrid, so that 48 V batteries are required. Therefore a total battery energy rating of 60 kWh, will have a required capacity of 1250 Ah. This battery capacity will be sufficient to enable a fully loaded battery to run expected loads for two days, at 10 hours a day, without recharging. For a one day system autonomy, battery capacity of 625 Ah is required.

Equation 4.1 is an expression used to formulate the battery capacity.

$$Battery\ Capacity\ (Ah) = \frac{(Average\ daily\ energy\ requirement) \times (Days\ of\ autonomy) \times 2 \times 1.5}{(Nominal\ battery\ voltage)} \qquad (4.1)$$

4.6. Solar panel environmental effects and location of use

Figure 4.1 shows the insolation map of South Africa (GeoSun Africa, 2015). Insolation is referred to as solar radiation (irradiance) received over a given period of time and is expressed in kWh/m². Whenever a PV system is designed, a location generation study can be made if the insolation and PV panel efficiency and performance parameters are known.

The eastern coastal areas in South Africa show moderate irradiation levels with an average of 1600 kWh/m², whereas the area around Upington, have values in excess of 2300 kWh/m². Horizontal sun insolation measurements have been made which means that the sun is in a

perpendicular orientation to the unit test surface on which the irradiance is measured. The map indicates the annual average amount of energy available from the sun via irradiation per square meter.

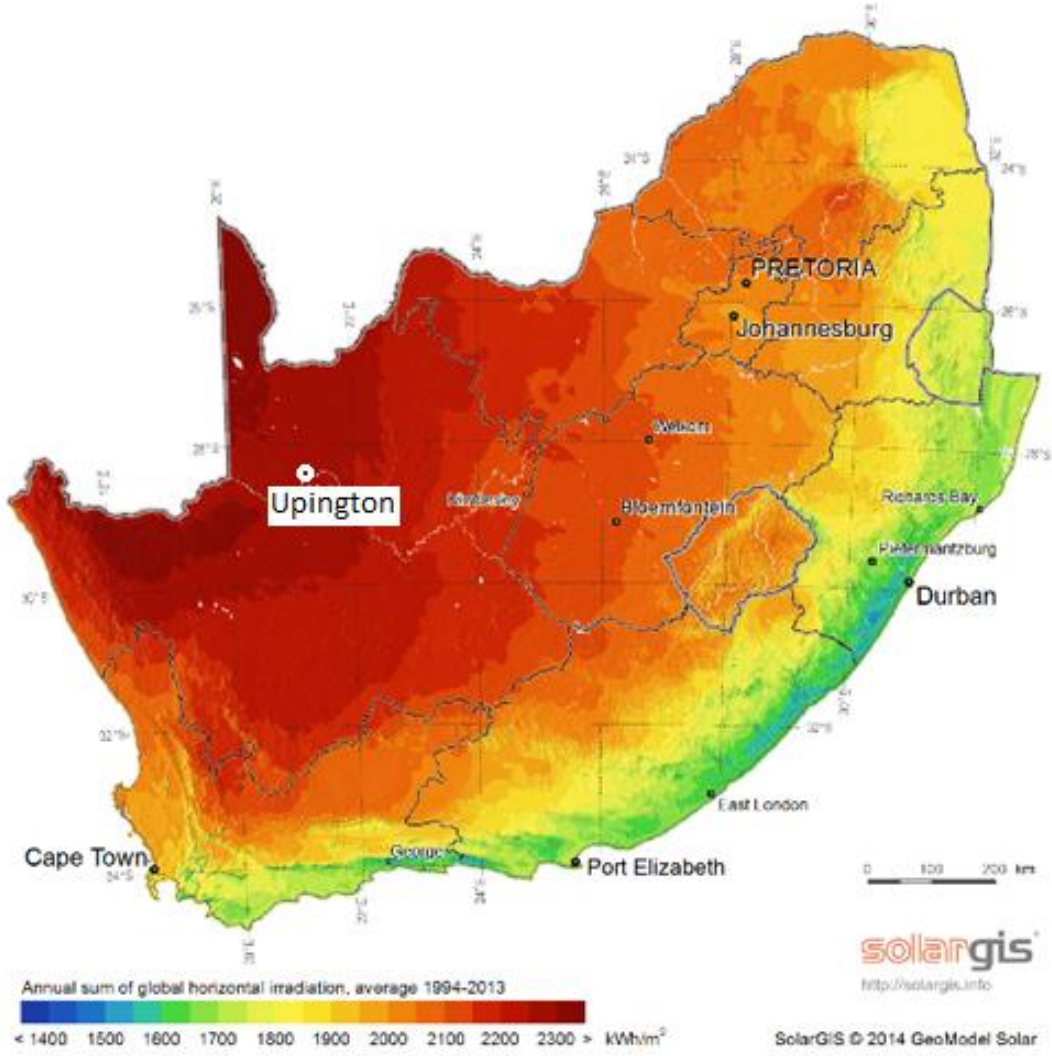

Figure 4.1: South Africa geographical insolation map (GeoSun Africa, 2015)

4.7. Sizing PV panels to meet system battery requirements

This section describes how PV panels are chosen for a system to meet the battery requirements. System designs can vary with panel voltage ratings. Common voltages to choose from are 12 V; 24 V; and 48 V. These panels can be configured in such a way that the optimum design is achieved.

The Solare PV panel with specifications as shown in Table 4.1 was chosen for this investigation. The maximum power voltage indicates that this panel will provide 47.5 V, which is suitable for a 48 V microgrid bus system.

Table 4.1: Solare Panels, 48 V, 350 W – specification (adapted from Solare 2015)

Module specification	Description
Model number	SM 350(40) P 1946×1315
Module Type	Poly
Maximum power (P_{max})	350 W
Open circuit voltage (V_{oc})	59.37 V
Short circuit current (Isc)	7.96 A
Maximum voltage (V_m)	47.5 V
Maximum current (I_m)	7.37 A
Maximum system voltage	1000 V DC
Operating temperature	- 40 °C to 85 °C
Module size (mm)	1946 × 1315 × 50 mm
Mass	35 kg
Material	Polycrystalline silicon
Number of cells	96
All technical data at standard test condition: Air mass unit = 1.5, Irradiation = 1000 W / m², Cell temperature = 25°C	

Figure 4.2 shows the average daily sunlight and daylight hours in Cape Town for each month of the year (Back to the source, 2015).

Sunshine & Daylight Hours in Cape Town, South Africa

- Mean sunshine hours in Cape Town range from 5:42 each day in July to 11:05 each day in December
- The longest day of the year is 14:15 long and the shortest day is 9:44 long.
- The longest day is 4:31 longer than the shortest day.
- There are an average of 2993 hours of sunlight per year (of a possible 4383) with an average of 8:11 of sunlight per day.
- It is sunny 68.3% of daylight hours. The remaining 31.7% of daylight hours are likely cloudy or with shade, haze or low sun intensity.

	Jul	Aug	Sep	Oct	Nov	Dec	Jan	Feb	Mar	Apr	May	Jun	Annual
Average Sunlight Hours/ Day	05:42	06:25	07:12	08:54	09:54	11:05	10:54	10:24	09:05	06:54	05:54	06:00	08:11
Average Daylight Hours & Minutes/ Day	10:07	10:54	11:56	13:01	13:55	14:21	14:07	13:22	12:22	11:17	10:22	09:55	12:00
Percentage of Sunny (Cloudy) Daylight Hours	57 (43)	60 (40)	61 (39)	69 (31)	72 (28)	78 (22)	78 (22)	79 (21)	74 (26)	62 (38)	58 (42)	61 (39)	68 (32)

Figure 4.2: Sunshine & daylight hours in Cape Town (Back to the source, 2015)

To estimate the size of the solar array, the system power requirements must first be determined and for how many hours in a day the system will be required to supply and meet the load demand. There are many guidelines in industry enabling the PV designer to plan and build such a system.

This next example will be used to explain the method used for sizing the PV panels of a system for one day autonomy on one house unit.

In December, during the summer months, the average daily sunlight is 11.1 hours, while shortest daily average of 5.7 hours occurs in July. First the daily battery capacity requirements is taken from Section 4.5. In this case the 625 Ah unit is considered. Then the sun hours that are available for a day must be determined. Note that the month with shortest average daily sunshine hours be considered; this will ensure that the system will receive an adequate charge in winter.

To get the total current rating required from the PV array, the one day autonomy 625 Ah value is divided by the shortest average daily sunlight which give 110 A .

Next the number of solar panels required, needs to be calculated. Take the current rating required from the array, and divide it by the current rating of the panel. The maximum power current specification in Table 2 of 7.37 A is selected. The result is 14.7 units and is rounded up to 15 panels.

The 15 PV units will be connected in parallel so that the total current will be 110, 6 A under peak conditions. The 15 panels as calculated meet the requirements of one house; for three houses and array of 45 panels all in parallel would therefore be needed.

4.8. Solar panel tracking

Tracking systems ensure that the solar collecting surfaces are always perpendicular to the rays of the sun. This configuration ensures most efficient energy absorption. Light sensitive resistors on the sides of a PV panel receive light and this information is used to control mechanisms which are able to rotate the pitch and tilt angle of the panel to the sun. When a full sun day is at its end, then the whole array will be re-aligned to face the east, in preparation for the following sunrise. Panel tracking should not be confused with maximum power point tracking (MPPT), which is explained in the next section.

4.9. Maximum power point tracking charge controllers

There are current technological advances which can enable PV panels to work at their peak performance. Temperature and other ambient conditions provide undesirable conditions for PV panels to operate in. An MPPT controller is used to make adjustments, based on the input received from the PV panels and provide a controlled output charge signal to optimise energy collection by the PV panels. These controllers also protect the battery from being over-charged.

According to the brochure by Solar-Electric (2015), an MPPT controller does digital electronic tracking. The outputs of the panels are monitored by the charge controllers and compared to the battery voltage. These controllers then calculate what the maximum power point would be for the panel output to charge the battery. This controller takes this power and converts it

to the most suitable voltage to charge the battery to its maximum capacity. Most modern MPPT controllers are around 93–97% efficient in the conversion of panel output to battery input (Solar-Electric, 2015). Typically a 20–45% power gain in winter and 10–15% in summer can be achieved. The gain is dependent on the weather, temperature, battery state-of-charge, and other factors such as cable resistance and lengths between the PV modules and the charge controller.

An example is provided to illustrate the operation of an MPPT controller as set out by Solar-Electric (2015).

Consider a 130 W solar panel a voltage of 1.6 V and a current rating of 7.4 A. The power of the panel, 130 W, is equal to the voltage multiplied by the current rating. The calculated 130 W does not equal the real 130 W delivered to a regular charger onto the batteries.

Should the voltage be 12 V, the power of the panels reduces to: 12 x 7.4 = 88.8 W; resulting In a power loss of 41.2 W for the 130 W PV panel. Because there is a poor match between the panel and the battery, inefficient charging will take place.

A panel that is rated at 130 W will only deliver this power value if it is subjected to insolation while the panel temperature does not exceed 25°C. If the temperature of the solar panel is higher than this, it will be very difficult to produce 17.4 V. At the temperatures seen in many hot climate areas, production might even be less than 16 V. It is therefore important to note that panels should not be undersized to the system voltage levels. PV panels should be configured to deliver the correct operating range of voltage and current to be combined with the charge controller.

4.10. Operation of MPPT charge controllers

The MPPT controller works as a high frequency DC–DC converter. It takes the DC output from the solar panels, changes it to high frequency AC, and converts it to a different DC voltage and current to exactly match the panels to the batteries. High frequencies around the 20–80 kHz range are present during these conversions. The advantage is that these circuits are designed with high efficiency transformers and components.

After the conversion process, the output regulator sends the output to the batteries. The charge controller manages the charge process taking account of variations in weathers, voltage changes, current changes, and temperature changes affecting the PV modules.

With reference to Figure 4.3, the following example of a 75 W PV panel has been used to explain power tracking functionality with a 12 V battery (Solar energy explorer, 2015).

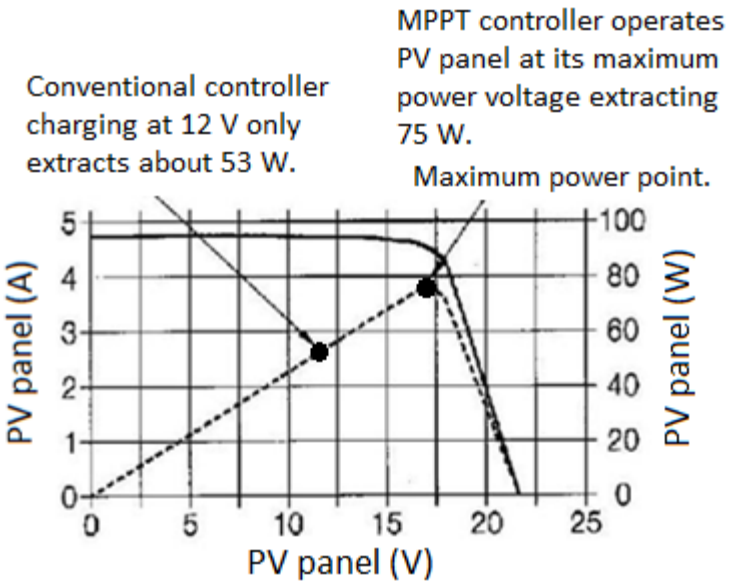

Figure 4.3: I-V Curve, PV power graph of PV panel, MPPT (Solar energy explorer, 2015)

A conventional charge controller simply connects the solar panel directly to the 12 V batteries. Thus the solar panel is forced to operate at 12 V. Direct connection between the panel and battery can also be thought of as clamping the DC battery directly to the PV panel. By connecting the 75 W panel to the 12 V battery, the conventional charger naturally reduces the power production by about 52 W. MPPT charge controllers compute the voltage at which the solar panels are able to produce the most amount of power at the maximum power point.

The maximum voltage of the panel is 17 V. The MPPT system thus operates the solar panels at their designed 17 V to obtain the full power of 75 W, despite the voltage of the connected battery. The battery charger voltage is higher than the battery voltage and can thus let current flow through the battery to supply charge.

4.11. Photovoltaic cell operation

A PV cell as depicted in Figure 4.4, works as a DC generator powered by the sun. When light photons of sufficient energy hits a solar cell, electrons are freed from the silicon crystal structure, and if there is an external circuit connecting the two semi-conductor plates of the cell, these freed electrons will be forced to flow through it. The voltage output from a single crystalline solar cell is about 0.5–0.8 V (Salmi et al., 2012). The amperage output of 7 A is directly proportional to the surface area of approximately 15 cm^2. Typically 36–72 cells are wired in series in each solar panel. This produces a 48 V nominal output for 72 cells (~ 55 V at peak power) that can then be wired in parallel with other solar panels to form a solar array to charge a 48 V battery bank.

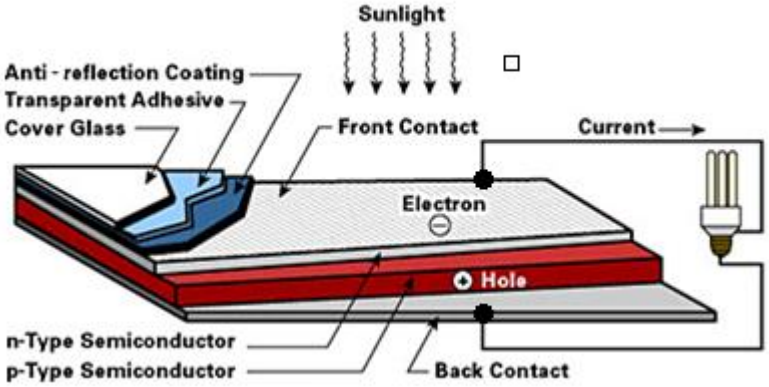

Figure 4.4: Photovoltaic cell (Btekenergy, 2015)

4.12. Solar cell efficiency

In 2012 three major families of PV cells were very popular, namely: monocrystalline technology, polycrystalline technology, and thin film technologies (Salmi et al., 2012). Monocrystalline cells have an efficiency of 10–15% efficiency, while polycrystalline cells have an efficiency of 9–12%. The thin film cell technologies have an efficiency of 9–12%.

At the end of 2014 it was announced that a new record for the conversion of sunlight into electricity has been established in Europe (Cleantechnica, 2014), after a four-junction cell solar cell developed through a French-German collaboration, achieved an efficiency of 46%, up from a previous record of 43.6%. The next expected efficiency potential is set as high as 50%, operating under concentrated sunlight.

5. MAS ALGORITHM DEVELOPMENT

5.1. Introduction

To describe the different aspects within the system as well as to describe functionality, the Matlab software model was developed in sub-components. The different function blocks fit together in order to merge the different area types together. The model is divided into physical power circuits and signal circuits.

Power circuits form part of the generation and delivery of electric power to the storage batteries and grid loads. These type of power circuits also include the switching devices, load components, as well as the photovoltaic generation blocks.

The second of programming block consists of lines identified as part of the signals and do not represent physical lines. These circuits function in response to the result or output of the calculations. Programming blocks include calculation blocks that consists of analog and digital signals. The logic is combined to simulate and execute the algorithms.

Figure 5.1 the Matlab program overview. Each block is a subsystem that is described and analysed in this chapter, to show how it functions.

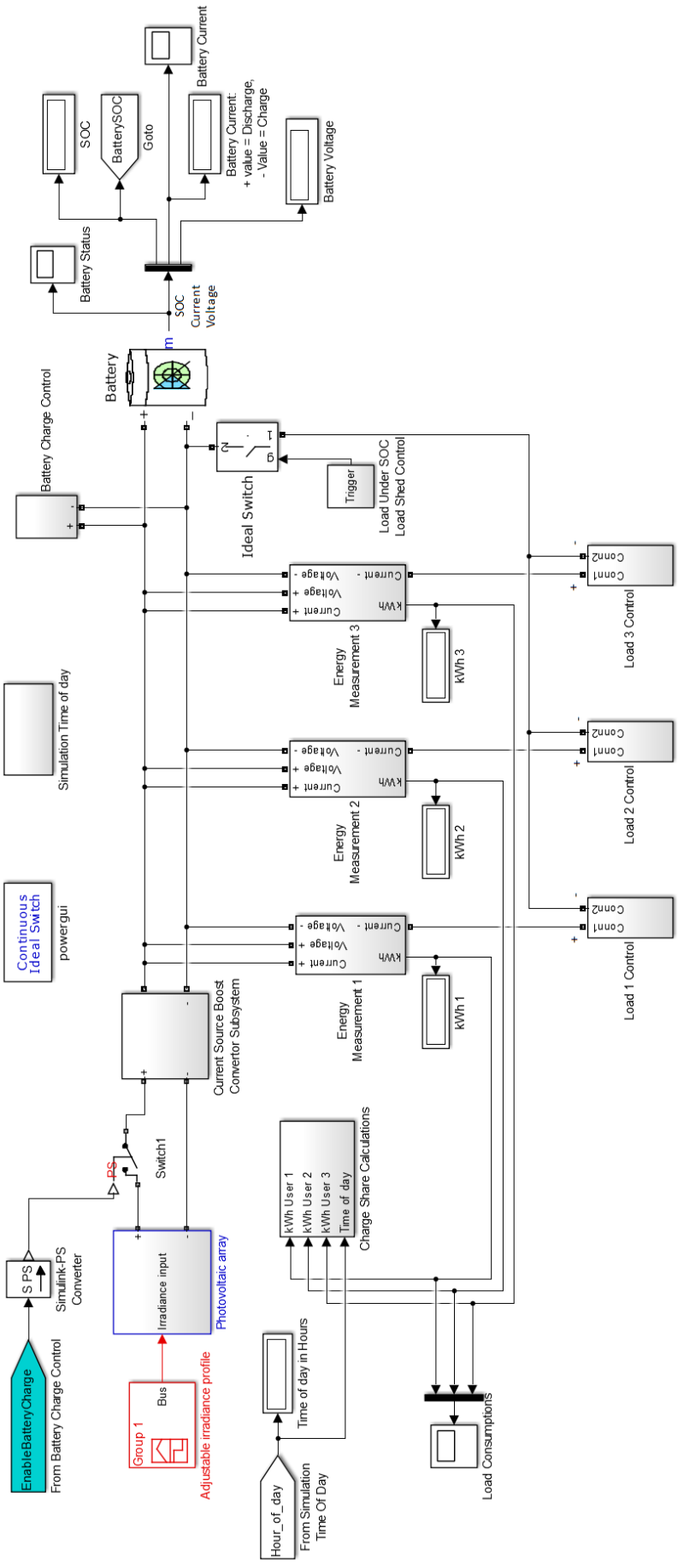

Figure 5.1: Matlab model overview

5.2. Time functions, simulation time

In order to simulate the time of day, a time base is required, to which all the time-related blocks can be coupled. A time 'Clock' block generates the time in seconds for the model. For every second the clock generates and inputs a pulse into the model.

The clock runs for a full day which is 86400 seconds, and from time zero generates a pulse per second, which is fed into the model; therefore over the course of a day the model receives 86400 pulses, between time 00:00 and time 24:00.

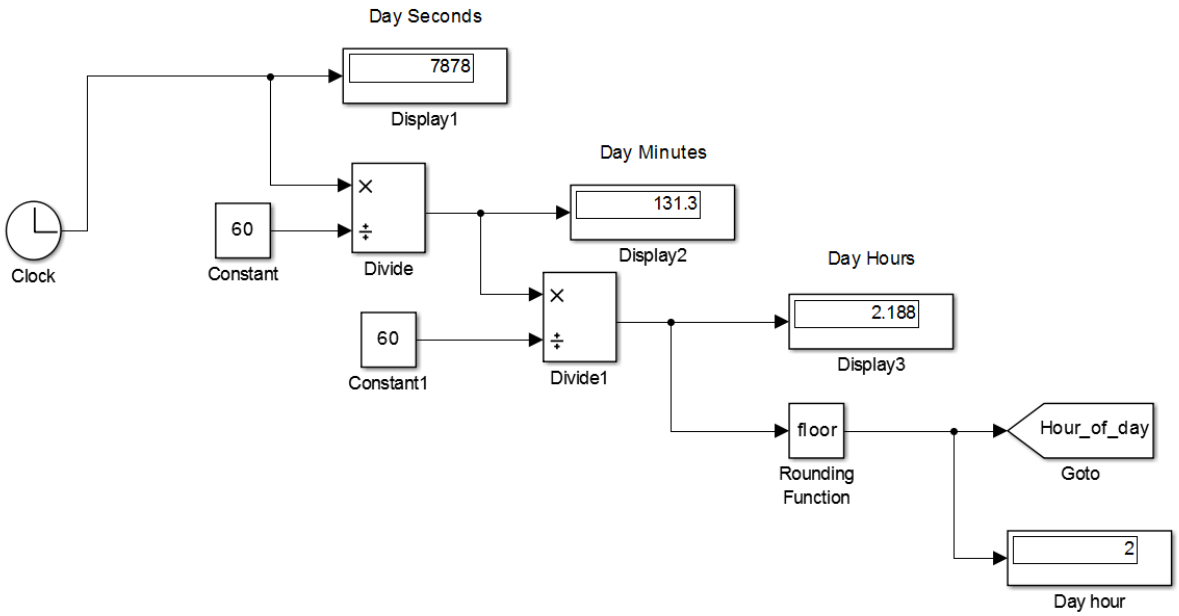

Figure 5.2: Simulation time functions

Simulated seconds are divided by 60 to generate minutes and minutes are divided by 60 to indicate the hour of the day. The hour time is rounded down to the nearest hour by the 'Rounding Function' block. The 'Rounding Function' holds the hour time value in order to use it as a reference hour value for various control blocks residing inside particular subsystems. Simulation time compared to real time speed is very dependent on the hardware system used to process simulated time in the model.

5.3. Adjustable irradiance profile

Figure 5.3 shows the ‘Adjustable irradiance profile’ block and the ‘Photovoltaic array’ subsystem.

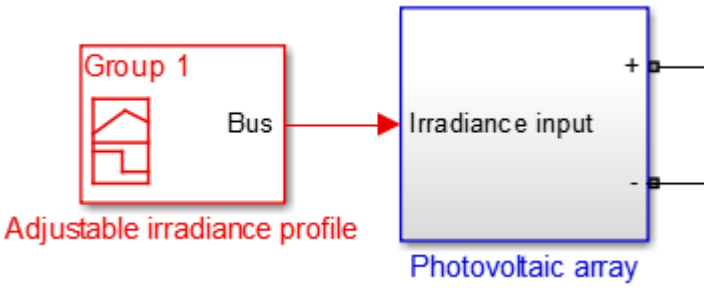

Figure 5.3: Irradiance reference signal builder for simulated PV array

In Matlab the ‘Adjustable irradiance profile’ block is referred to as a signal builder. Irradiation set points can be adjusted to any gradient required. The x-axis reflects the time of day from 0–86400 seconds (00:00–24:00) and the y-axis is the irradiance level in W/m².

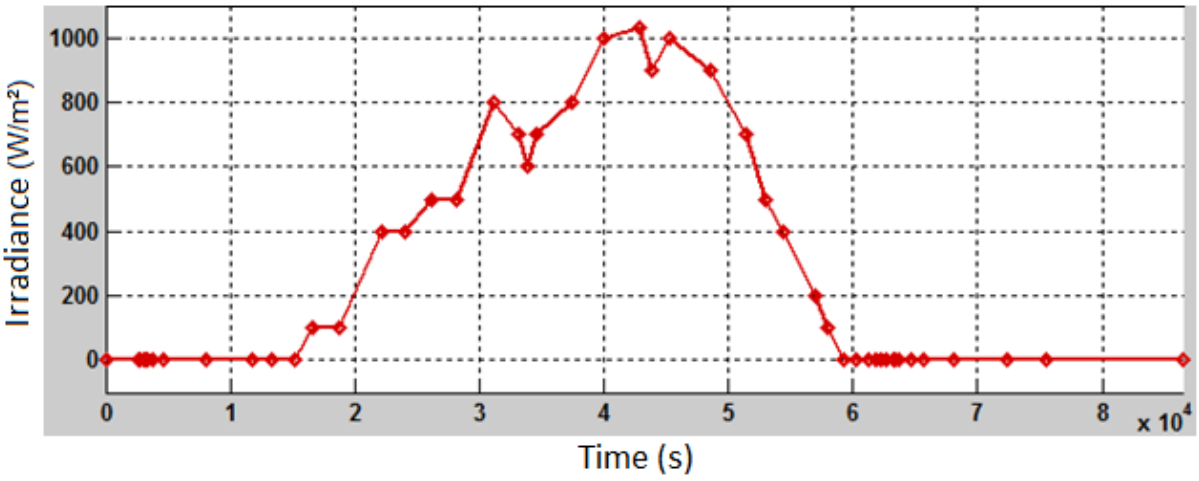

Figure 5.4: Adjustable irradiance reference profile for the simulated PV panel

Weather conditions can also be simulated; cloud effects and seasonal changes are programmable. The battery charge profile is dependent on the irradiance profile. The graph shown in Figure 5.4 shows the irradiance profile that is used as the reference for the simulated photovoltaic array. An infinite number of coordinates can be created and varied manually to adjust the profile before the simulator is started.

5.4. Photovoltaic array

Construction of the simulated photovoltaic panel inside the Matlab program consists of 72 solar cells connected in series and capable of delivering 48 V DC. The parameters of each individual cell can be set to change the voltage and current delivery from the panel depending on the irradiance reference supplied to the panel. Power delivery will be proportional to the irradiance reference.

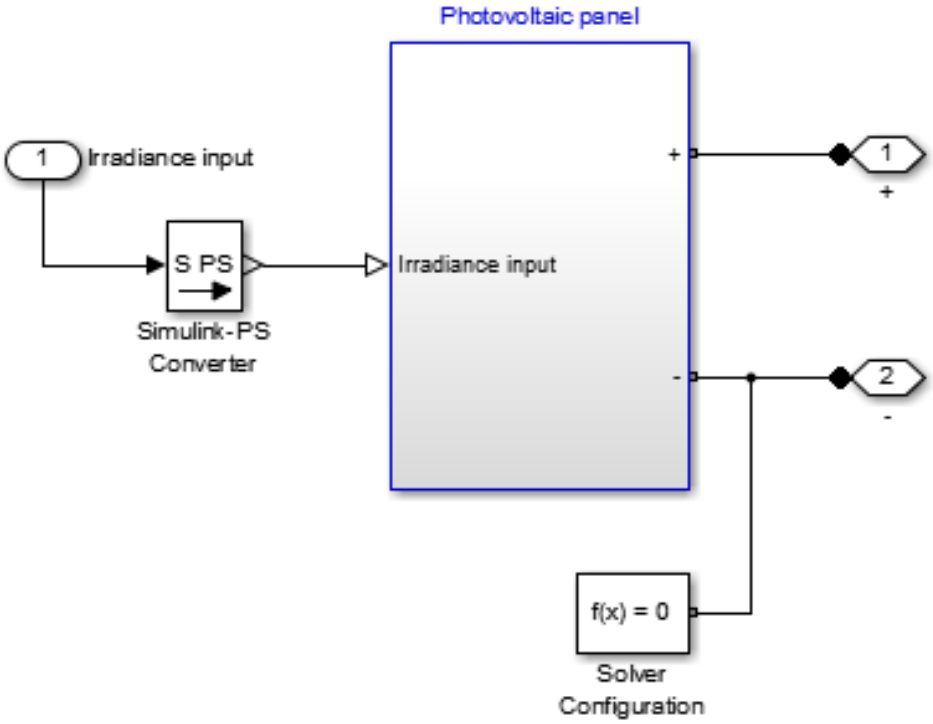

Figure 5.5: Photovoltaic subsystem

Figure 5.5 shows the subsystem for a PV panel and Figure 5.6 shows the solar cells within the subsystem.

Figure 5.6 indicates six of the 72 cells that forms part of the photovoltaic subsystem. Irradiance input contributes to the direct connection of reference irradiance to all the cells.

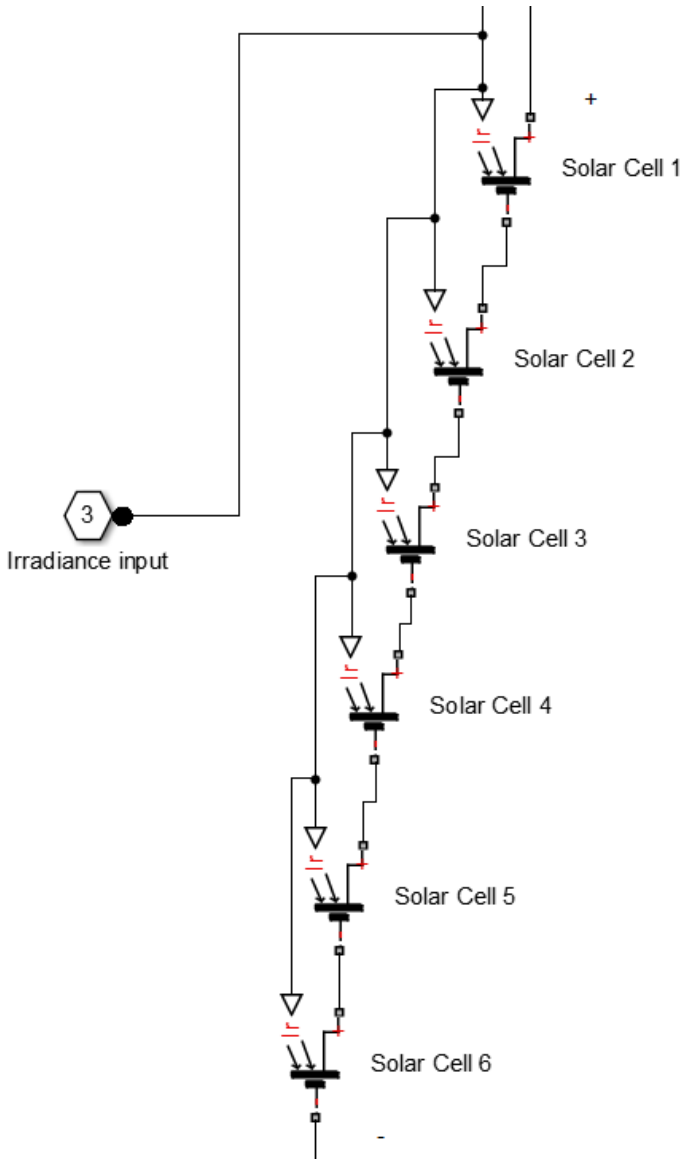

Figure 5.6: A diagram showing 6 of the 72 solar cells inside the simulated PV panel

5.5. Current source boost converter subsystem

Matlab does not allow direct connection of physical lines to signal lines. Physical lines represent items identical to physical items such as conductors and resistors for example. These lines can also be referred to as lines from the Simulink group and SimPowerSystems group type lines.

As indicated in Figure 5.7, the ‘PS-Simulink Converter 1’ block is thus required to connect physical and signal lines together. This will enable the passing of a signal line through the point of conversion and allow the same value to be carried over to the physical line connections.

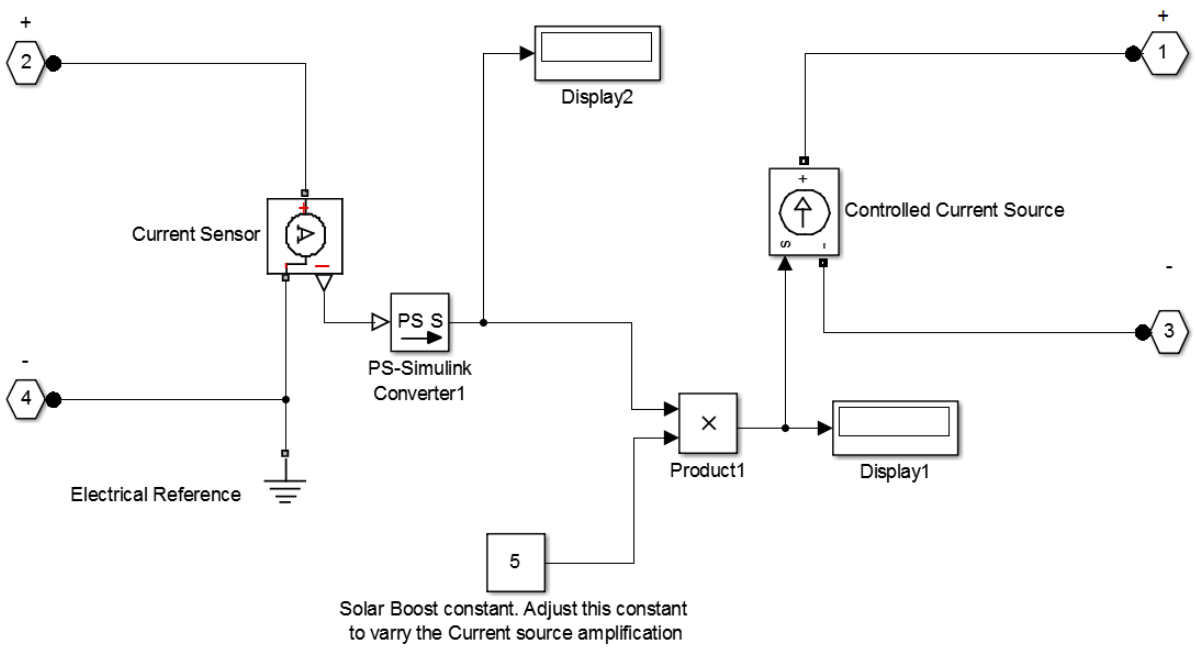

Figure 5.7: Current source boost converter block

A subsystem is a block that contains many other blocks inside it that forms a system. The current signal generated by the photovoltaic panel is connected to Terminal 2 and 4. This current is measured by the current sensor and the value is passed via the ‘PS-Simulink Converter 1’ to the ‘Controlled Current Source’ block.

The ‘Controlled Current Source’ will receive the reference signal on terminal 'S' and generate an equal current loop through Terminals 1 and 3. A product block ('Product 1') allows a user input to amplify or boost the current as represented by an increase in current if the simulated irradiance on the PV panel is increased; it is also possible to decrease the irradiance. The user thus does not need to build multiple photovoltaic panels to increase the current source reference because it can be adjusted by the boost constant.

5.6. Battery block

The battery block shown in Figure 5.8 is accessible from the electrical elements section under the SimPowerSystems group inside the Matlab software. The battery is used as the storage device. The model has three terminals that comprise of two physical terminals, and a third terminal having three internal status signals. The positive pole and negative pole of the battery are connected to the main DC bus of the microgrid model. Terminal 'm' consists of three signals: voltage, current and SOC.

When the irradiance reference level raises, the PV panel responds by increasing the electrical energy delivered.

A lithium-ion battery was chosen for the simulation. Battery types can be chosen from the options block on the Matlab dropdown options list.

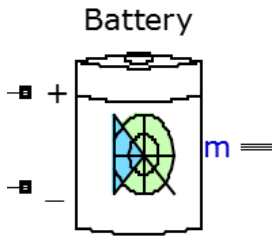

Figure 5.8: Battery block

Battery parameters can be adjusted within the battery model block shown in Figure 5.8. Nominal voltage is set to 48 V DC and this voltage level forms the basis of the DC bus. Battery capacity is adjustable through a capacity setting. The SOC setting of the battery illustrates the setting to the initial charge state of the battery when the model is started.

Figure 5.9 shows that the nominal battery capacity area of use is from 100–20%. Battery damage is prevented by disconnecting the battery from the load when the knee point is reached during discharge. The internal operation of the battery, namely charging and discharging, is simulated by the Matlab mathematical battery block. The SOC will be adjusted accordingly as battery charges and discharges.

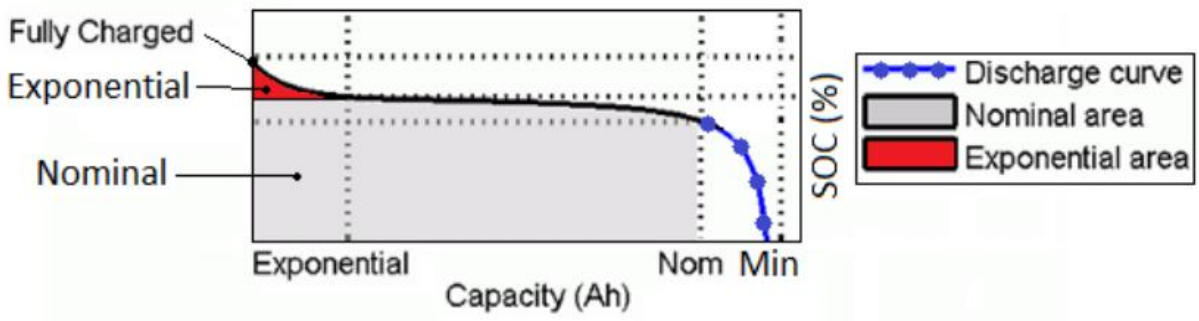

Figure 5.9: Typical battery discharge characteristics (Matlab R2014a)

During battery charge conditions, a negative current value as shown in Figure 7.1, is visible from the battery measurement point. Positive battery current shows that the battery is delivering energy to the loads and acts as the supply source.

5.7. User load control types

The user load control subsystem is divided into two control areas. The first area of logic provides user input to manipulate conditions when loads are operating. The second logic zone handles control through the external charge share control inputs.

Figure 5.10 depicts three load control blocks, sequentially numbered. All ‘Conn2’ terminals are connected to the negative DC bus. This DC bus is manipulated by the SOC ‘Load Shed Control’ unit. Each ‘Conn1’ terminal is connected to its respective power measuring block. Voltage to each load is obtained from the DC bus via the power measuring block.

Each individual load control block has a resistor inductor capacitor (RLC) component. For each load control, a power consumption value can be chosen by the Matlab user which will simulate the power used by the corresponding house at that particular time. This area of logic is referred to as the first type of load control where load parameters can be set.

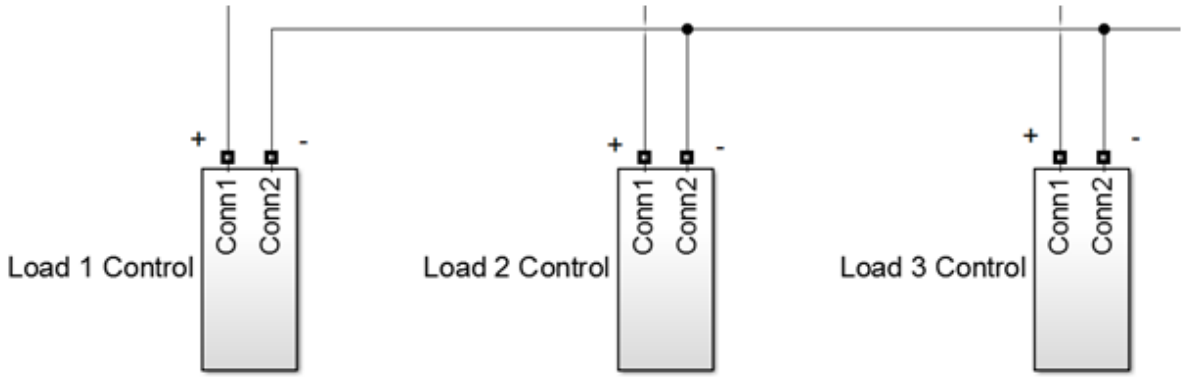

Figure 5.10: Load control blocks

Conditions are pre-set so that the model will emulate the random switching patterns of user loads. The result is a load pattern typically demanded by a home owner over a 24-hour period.

The second control area is adjusted from the ‘Charge Share Calculations’ block. During the course of the day, all the power supplied to a user is added to give the maximum power used every hour; these maximums are stored to provide a record of the individual consumption figures. When the load share time of 18:00 is reached, the load switch will be either kept closed or it will be opened. Switch operations are dependent on how much energy is reserved for a particular user as dictated by the SOC at load share time. When the model switches over to the reserve share state at nightfall (after 18:00) all the loads will be allocated in accordance with user's reserve share allowance energy values. Each user will be allowed

to draw power until his energy allowance capacity has been depleted, at which time the user will be disconnected from the grid.

5.8. Block operation

This section gives the functional block descriptions and the process flow of logic control.

Interval test functions are put in place to have input control over the time functions of different house loads. The Matlab user can use these functions to simulate the fixed loads for each house as a unit; individual loads for the different applications inside a house are not considered. If the load fluctuations from individual houses is required, then the necessary load control algorithms will have to be developed. Figure 5.13 shows the program inside 'Load 1 Control'. The simulator has three loads and will present three separate control areas for the three loads. Inside these areas of control there are two RLC loads; this demonstrates the dual function if more than one fixed load setting is desired.

The subsystem shown in Figure 5.11 begins with the 'Hour_of_day' transfer block. The time simulation is linked to this input and the time signal is directed to the 'Interval Test RLC 1' block units. These interval units hold the settings to select when the block should allow load switching. It possesses a rise time and a fall time setting that will react on the hour. Whenever a condition where the settings are within the actual timeframe, is met, a logical '1' will be passed to the 'OR' block for further processing. If no condition is met within this timeframe, then a logical '0' will result from it.

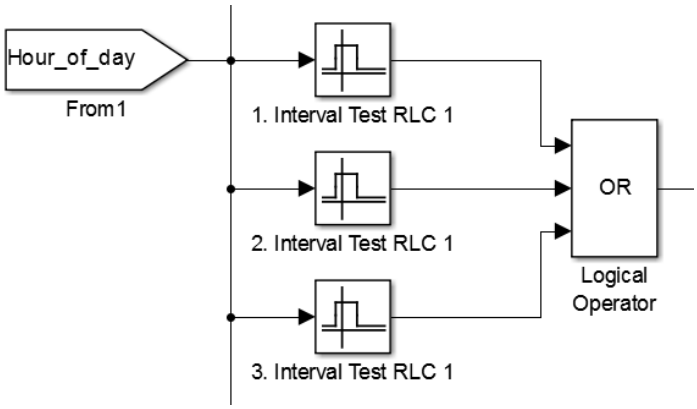

Figure 5.11: Interval test time input parameters

The interval units are connected in parallel so as to have adjustable multiple timeframe set points. RLC 1 settings have control over the Series RLC Load 1 and RLC 2 interval settings are linked to Series RLC Load 2.

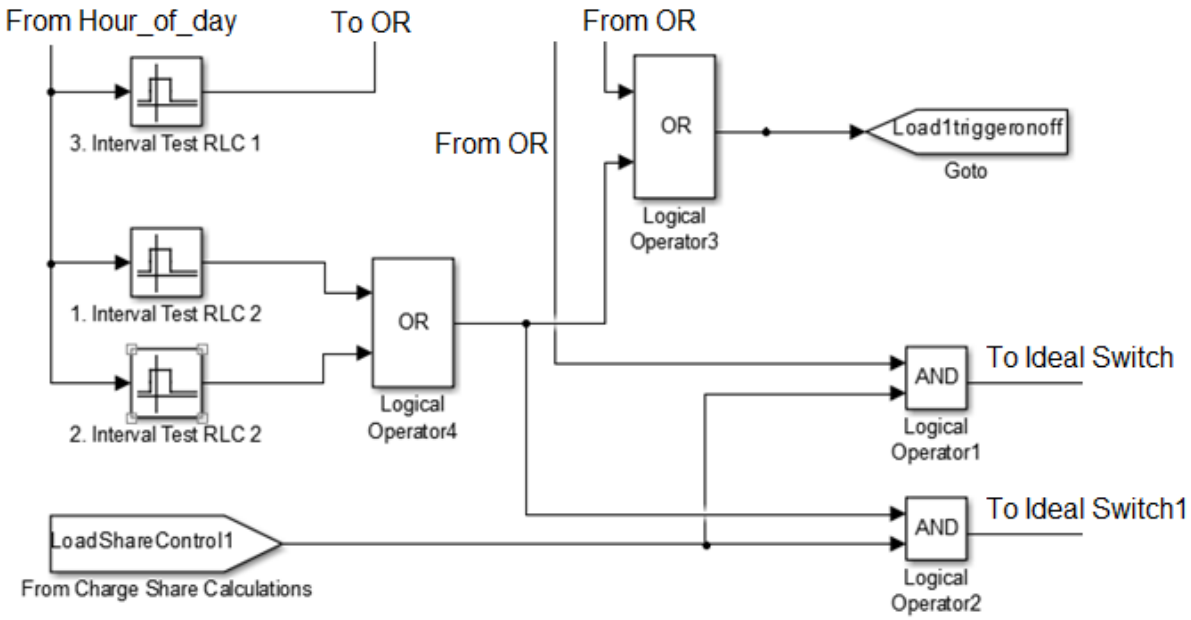

Figure 5.12: Load share availability load control

Load switching is enabled and disabled through the ‘Charge Share Calculations’ input block. The load share signal will pass a logical '1' to both the ‘AND’ blocks. The ‘AND’ blocks as shown in Figure 5.12, act as gates which control the switching signals obtained by the interval test units via the ‘OR’ function blocks.

The ‘OR’ block at the ‘Logical Operator 3’ location gives the ‘Load1triggeronoff’ link status, to show if any of the interval test units are enabled. Figure 5.13 displays each of 'Series RLC Load 1' and 'Series RLC Load 2' as a fixed load resistor. Ideal switches are triggered by the ‘AND’ logic block. Terminals '1' and '2' complete the DC circuit from the main bus through to the power measuring function and SOC load shedding control function blocks.

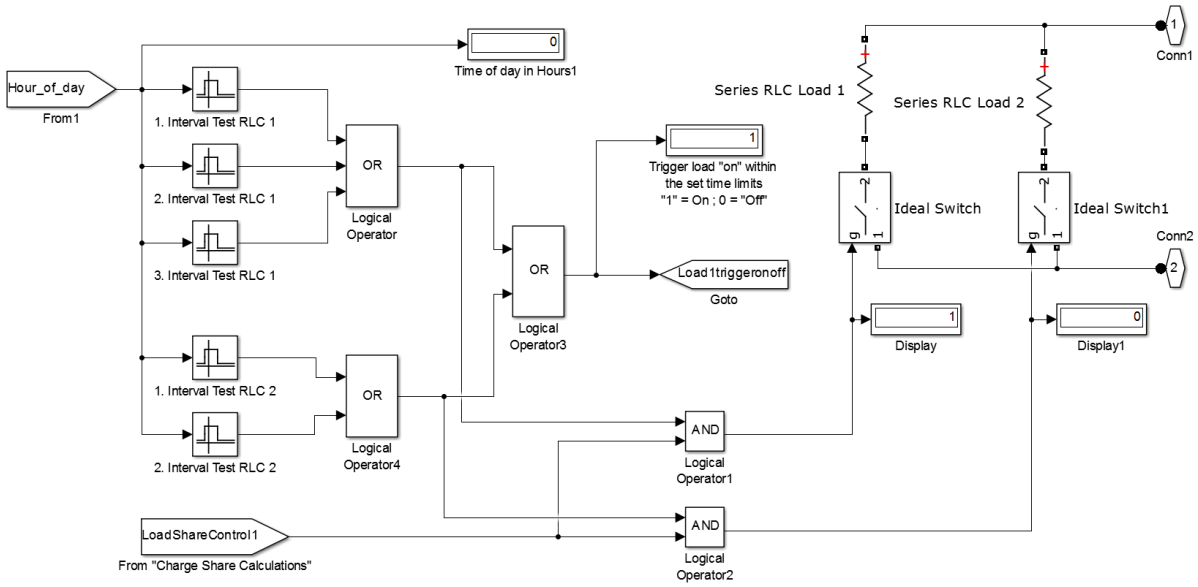

Figure 5.13: Load control logic

5.9. Battery charge control

In order to keep the battery at its peak delivery state, the model should always attempt to regulate the voltage within certain limits. The state-of-charge level will determine the amount of time and energy that will be allocated to the loads. The higher the SOC, the bigger the capacity of the battery, and the more power will be available to service consumer loads at night – ideally the SOC should be 100%. In model, limits of the SOC within the battery can be adjusted by the Matlab user via the 'Battery Charge Control' block. Figure 5.16 shows Terminals '1' and '2' which respectively transmit the DC bus voltage as a reference voltage.

By means of the ‘S-R Flip Flop’ block, charge control is switched 'on' or 'off'. The system design voltage operates on 48 V DC; if the voltage level drops below 45 V DC as in Figure 5.14, or the SOC falls below 70% shown in Figure 5.15, then the condition enabling charging will be processed. These limit parameters are adjustable by the Matlab simulation user.

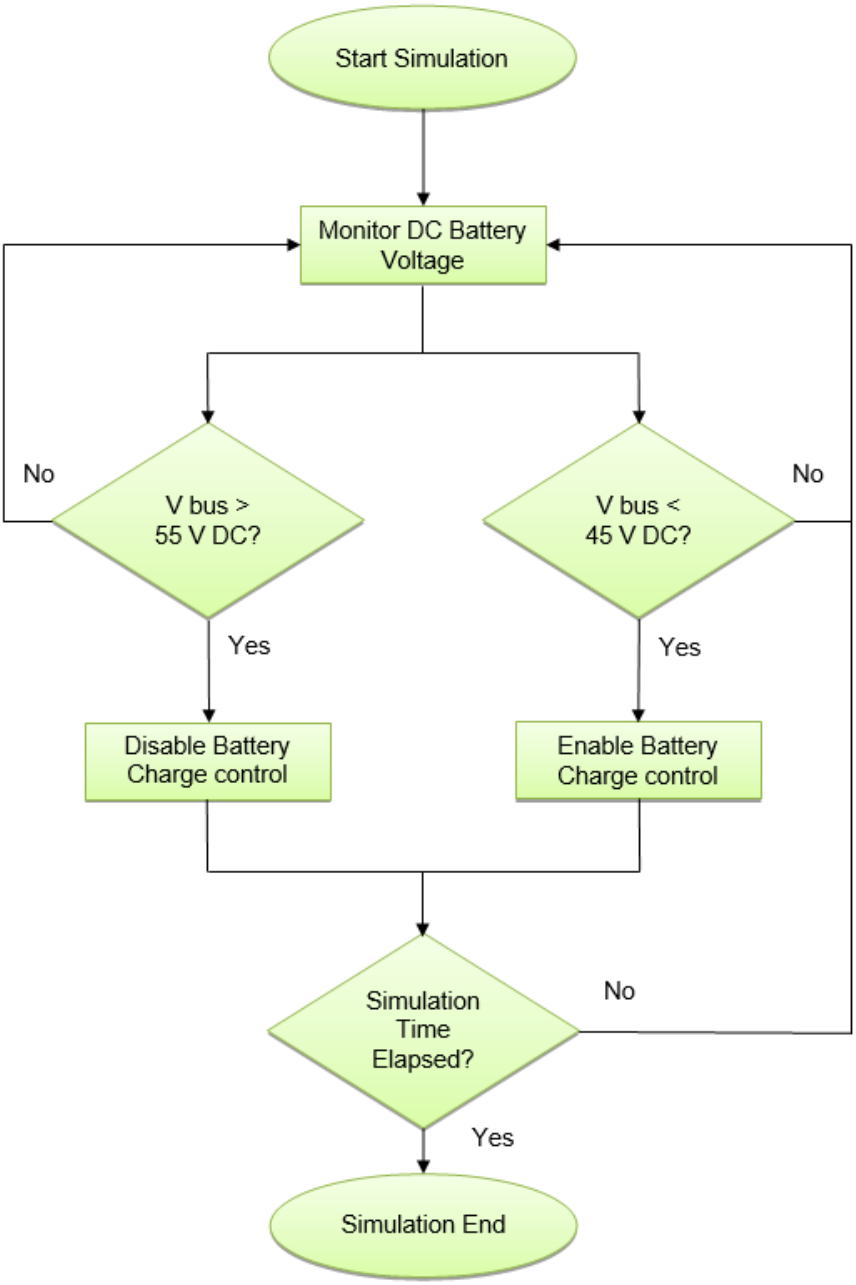

Figure 5.14: Battery charge control flow chart, voltage reference

'Battery SOC' is linked from Figure 5.1 to Figure 5.16 with the 'From' and 'Goto' invisible link. The 'S-R Flip Flop' block will latch and drive the 'Bit to Integer Converter' block. The converter block allows conversion of the signal types in order for the 'EnableBatteryCharge' block to receive this signal in its required format.

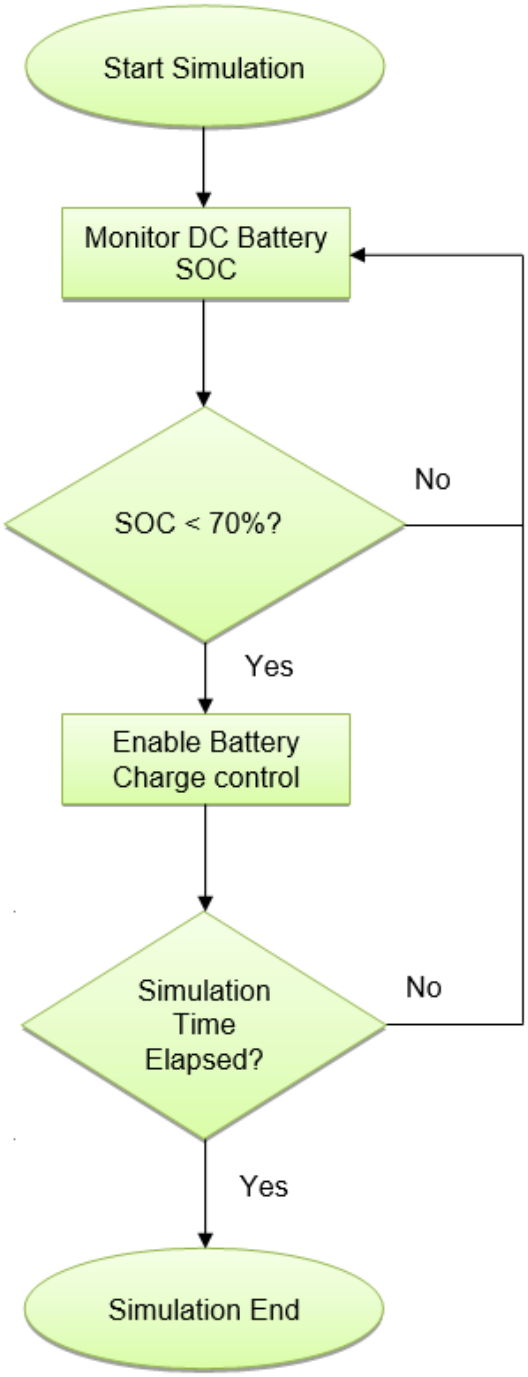

Figure 5.15: Battery charge control flow chart, SOC reference

Whenever the bus voltage rises above 55 V DC, or reaches the user input limit shown in Figure 5.16, then the ‘S-R Flip Flop’ will unlatch to disable charging to the battery.

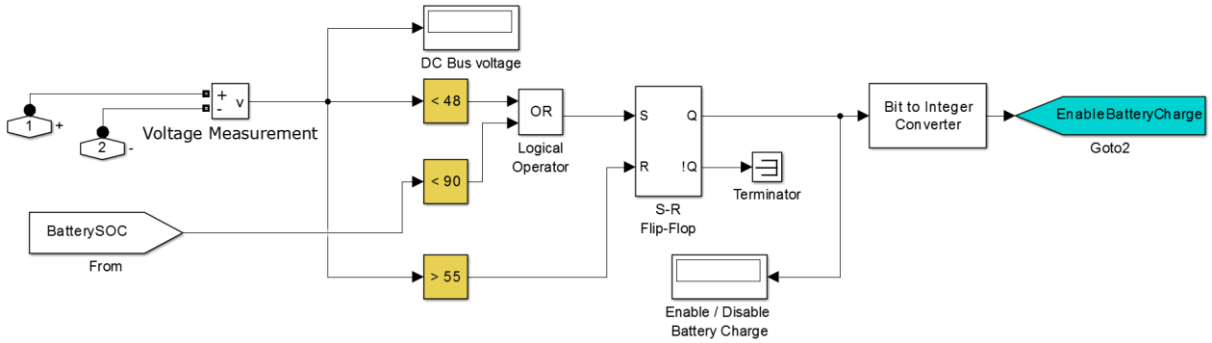

Figure 5.16: Charge control logic

Figure 5.17 illustrates the in-line control 'Switch1' situated after the photovoltaic array subsystem. Command is transferred to 'open' or 'close' to the control limits as given by the control logic the control logic.

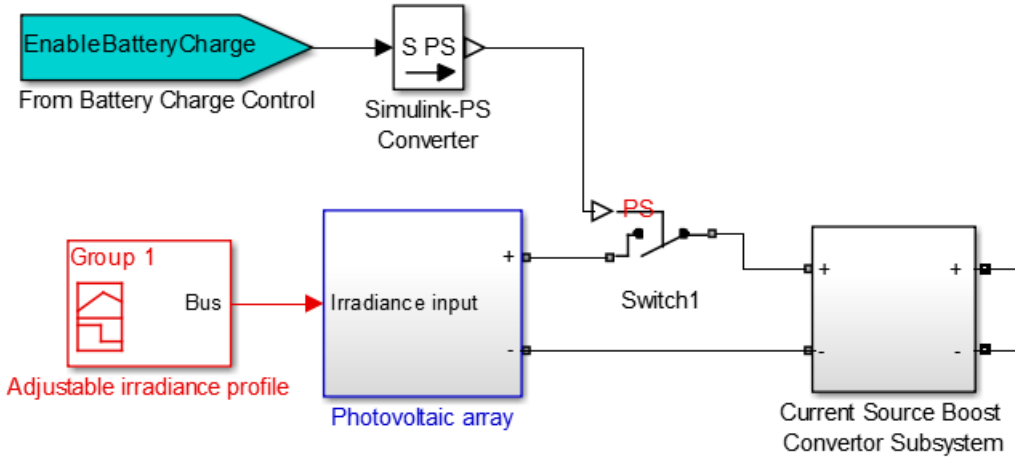

Figure 5.17: Charge control switch

'Switch 1' in Figure 5.17 is controlled by the 'EnableBatteryCharge' block via the 'Simulink–PS Converter'.

5.10. Energy measurement

In the following section the operation of load energy measurement will be explained. Load measurement of 'load 1' is referred to. The power consumption of each load needs to be monitored and recorded each day. Measurement will start at time, 00:00.

The value of each load is held at its maximum consumption value. At 18:00 the 'Charge Share Calculations' Block in Figure 5.1 will deal with the load shedding values as received from the 'Energy Measurement' block. The 18:00 time stamp is chosen as a default time for

sunset. Irradiance levels will to go down to zero at this time which is set by the Matlab user. Batteries will not be charged after this time and energy will selectively be transferred from the batteries to the loads via load control. In running the simulation, the Matlab user can change the sunset time and the irradiance effect on the charging of the battery. The battery provides the reference voltage to the DC bus.

The loads are fed through the ‘Energy Measurement’ blocks to measure energy consumption. This will be the energy drawn in that specific moment in time. A time factor should also be considered when energy values are compiled.

5.11. Energy measurement block operation

Figure 5.18 introduces the subsystem that will be responsible for energy measurement. Each load has its own respective energy measurement block (annotated as 'Energy Measurement' in Figure 5.18).

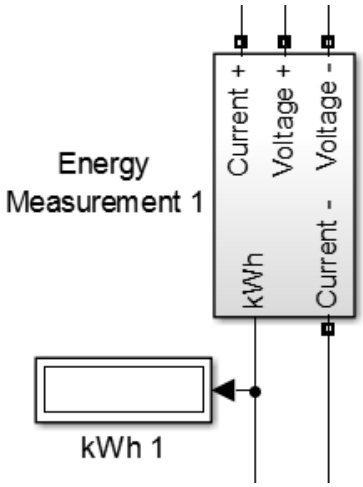

Figure 5.18: Energy measurement

Terminals '1' and '2' in Figure 5.19 are the respective inputs and outputs for current measurement. The positive terminal is directly connected to the DC bus and the negative signal routes current flow towards the load blocks. Terminals '3' and '4' connect to the positive and negative conductors of the DC bus respectively. The ‘Current Measurement 1’ and ‘Voltage Measurement’ blocks measure and relay the measured signal the product block.

In the next part of this section an explanation of how timing is controlled in relation to switch times and the 'on/off ' commands whenever energy measurement is active.

Whenever a load is activated during the day, an enabled signal will be sent via the ‘Load1triggeronoff’ block. The function of this block is to link it to ‘Load 1 Control’, as shown in Figure 5.10; Matlab uses this function to connect signals between two points, without using wiring.

A ‘Pulse Generator’ is used where the load-enabled signal is joined through an ‘AND’ block. The ‘Pulse Generator’ will produce a pulse to simulate a second of clock time. For every second that a load is active, a digital pulse will be produced, and these pulses are added by the 'Counter' block. When a load becomes inactive the total number of pulses summed by the counter, represents the time in seconds that the load was active. The sum is the total seconds of operation, which is then converted to hours.

The value of the load (kW) is then multiplied by value of the time (hours) over which the load was active, to produce energy (kWh) used. The ‘MinMaxRunningResettable’ function block takes this value and passes it on to the ‘Discrete Sample & Hold’ block. The ‘MinMaxRunningResettable’ block ensures that the energy used is retained in memory when the load is switched off and on again. Without this function the ‘Discrete Sample & Hold’ block cannot retain values that should be continuously added up as load conditions change from active to non-active. A constant of zero is applied to the reset input of the ‘MinMaxRunningResettable’ block, to disable reset functionality.

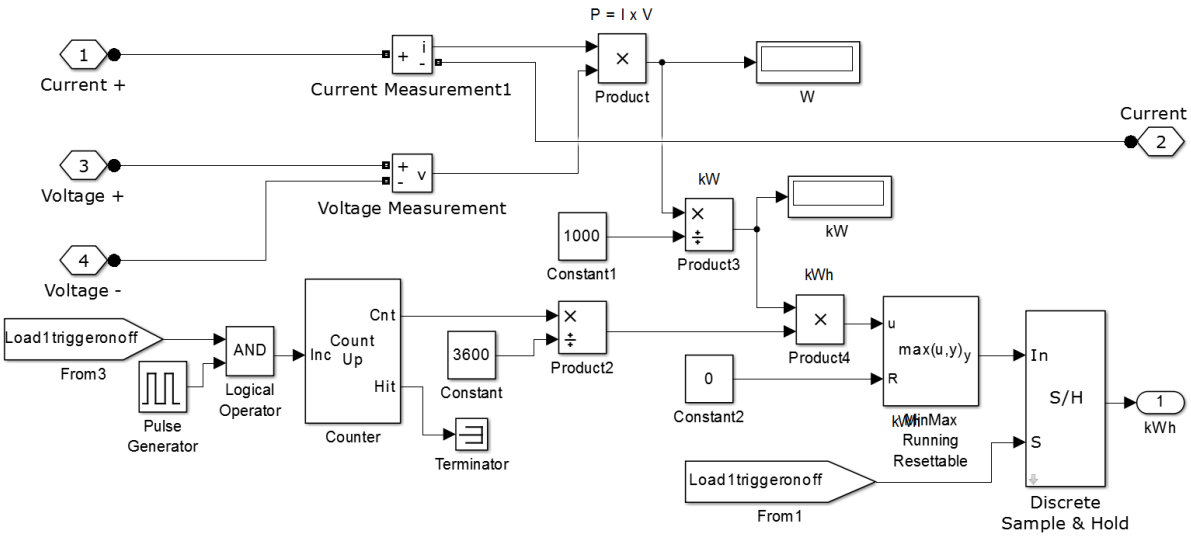

Figure 5.19: Energy measurement logic

‘Discrete Sample & Hold’ is activated only when energy is being consumed. The energy value that is held by the ‘Energy measurement’ block is passed to the ‘Charge Share Calculations’ subsystem via the directly connected Terminal '1'.

5.12. SOC load shed control

Total battery discharge needs to be prevented. When the SOC goes down, a limit of 20% shown in Figure 5.20 as setup by the Matlab user, will introduce a condition where all the loads will be disconnected from the grid. If this condition is met, then the battery is considered to have been drained. Battery charging will be controlled by the 'Battery Charge Control' block shown in Figure 5.1. When battery SOC reaches 50% the 'Set-Reset' block will latch to allow loads to be connected to the grid again.

Users of the model have access to adjust these limits. In practice it is not advisable to drain the battery below a SOC of 50%. In this model these limits can be adjusted to any value from 0–100% as required to observe how battery discharge reacts with the loads.

The 'Terminator' block is used to connect unused terminals on function blocks; this is done prevent potential errors arising from open-ended terminals. The 'Bit to Integer Converter' allows connection and signal type conversion between Terminal '1' and the output terminal 'Q', of the 'S-R Flip-Flop' block.

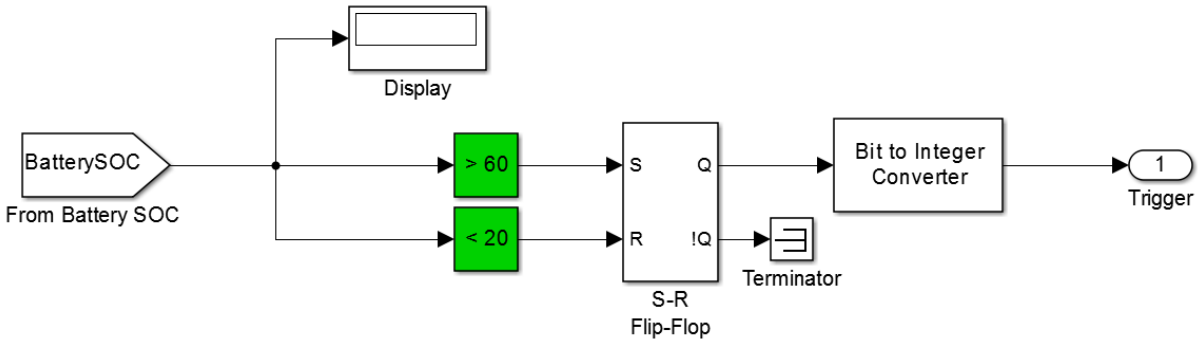

Figure 5.20: Load under SOC load shed control

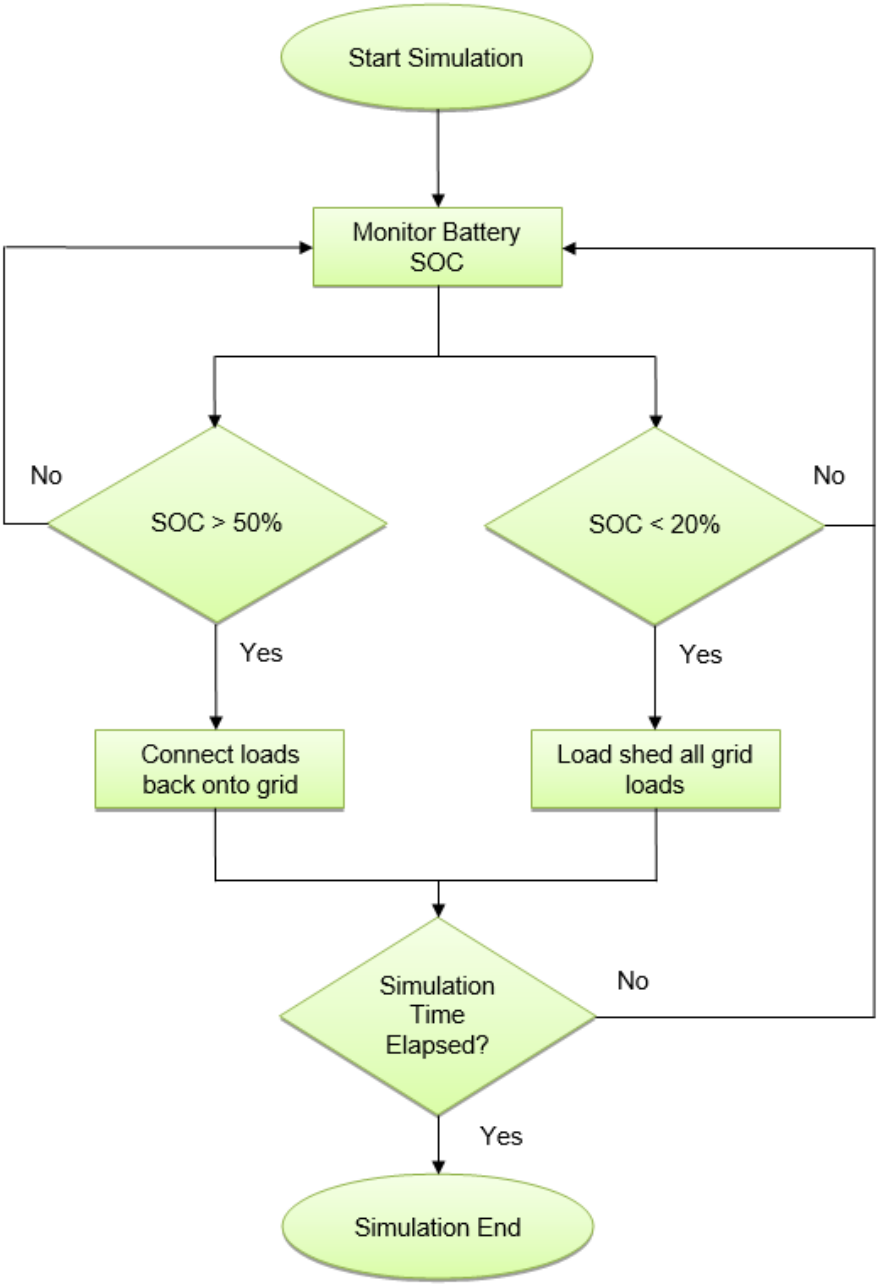

Figure 5.21: Flow chart of load control subject to battery SOC

5.13. Charge share calculations

A reserve share formula has been derived and is explained in detail. The subsystem is disassembled to explain the internal working of the functional area. Section 5.13.1 explains the battery SOC to energy (kWh) conversion. Section 5.13.2 shows how the energy charge reserve shares carry out their function, and its technical logic breakdown is treated in Sections 5.13.3 and 5.13.4.

5.13.1. State-of-charge to energy (kWh) conversion

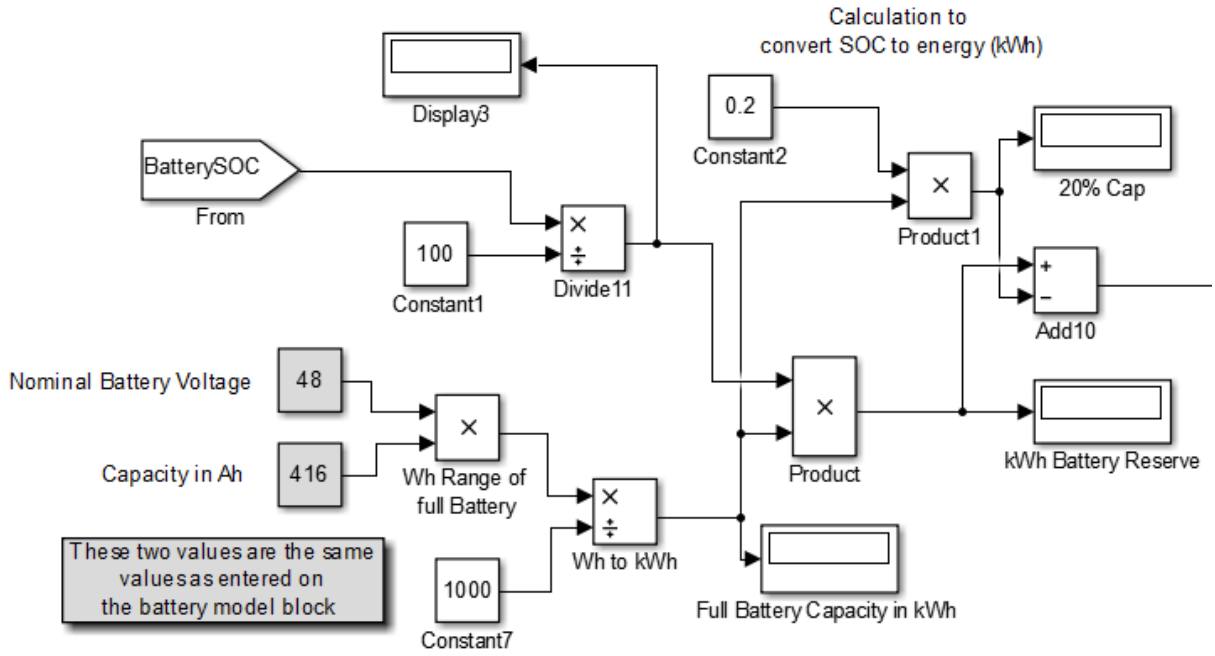

Figure 5.22: State-of-charge to energy (kWh) conversion

Before the model simulation is initiated, the user must confirm that the battery voltage and battery capacity parameters are inserted as selected from the 'Battery' block in Figure 6.1. Grey coloured blocks in Figure 5.22 are shown to indicate these user inputs.

Matlab does not provide an energy display (kWh) in the ‘Battery’ block. The state-of-charge of the battery is available from Matlab and therefore an SOC to electrical energy (kWh) conversion is done.

Multiplying the nominal voltage of battery by the rated capacity, yields the total electrical energy that the battery can hold. The total energy content of the battery is given by:

$$E_{Battery\ Total} = \frac{V_{Battery} \times Ah_{Battery}}{1000} \tag{5.1}$$

To determine the reserve energy capacity of the battery, multiply the total battery energy from Equation 5.1, by the SOC of the battery; this leads to Equation 5.2 below:

$$E_{Battery\ Reserve} = E_{Battery\ Total} \times SOC_{Battery} \tag{5.2}$$

For visual validation within this subsystem, a display function is active to monitor the state-of-charge levels. The battery is protected to not discharge below an SOC of 20%. Usable

battery SOC has already taken account of the 20% deduction from the battery full range; see Figure 5.23.

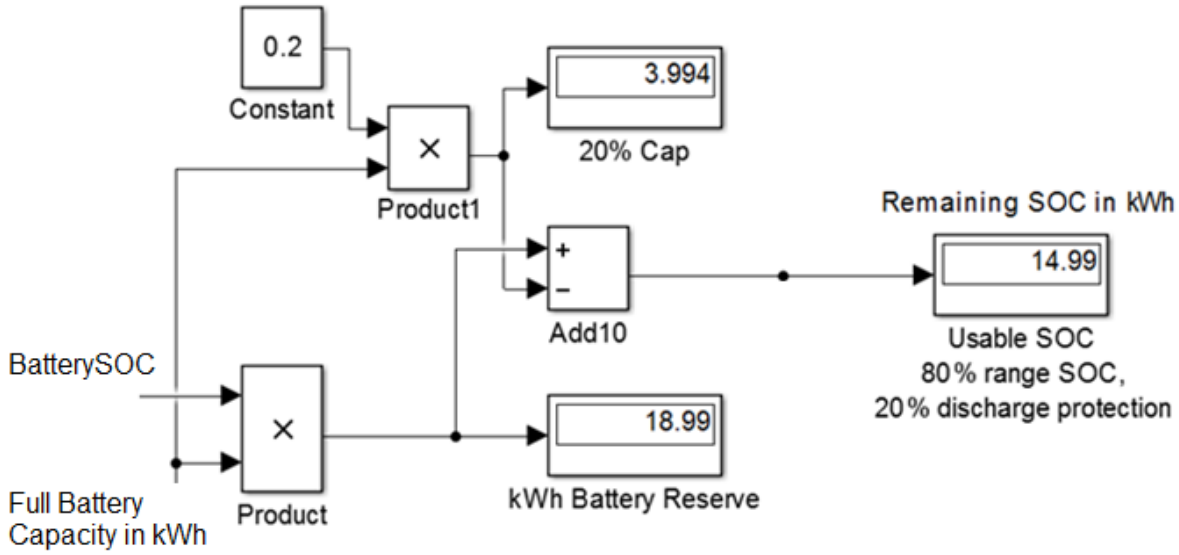

Figure 5.23: Battery reserve energy

5.13.2. Reserve share formulation

Formulation of the allocation from energy reserve is discussed for one user only. Each user within the system will have their own identical formula by which their proportion of the available energy reserve will be calculated. The stokvel concept will always ensure that the user with the lowest daytime energy consumption, is allocated the biggest portion of the available energy reserve through the night. Conversely, a user with a large daytime energy consumption, will have a small amount or even zero energy for night time use, available to him. A formula derived as Equation 5.3 below, allocates the energy reserve, taking account of a user's total daytime energy consumption in relation to the total daytime consumption by all the grid users. The amount of electrical energy available for night time distribution via this algorithm, will depend on the SOC of the battery at nightfall.

The subsystem will allow the respective loads to be either 'on' or 'off '. No stored energy will allocated until the designated time which is taken to be the end of the day in terms of power generation, is reached; in the case of the model under discussion, 18:00. When the limit of a user's allocation from the reserve energy stored, is reached, his switch will be opened and his load shed off the grid.

5.13.3. Reserve share logic

During daytime a summation process adds all the user energy consumption values and a running total is shown in the display 'Total kWh Used', as depicted in Figure 5.24.

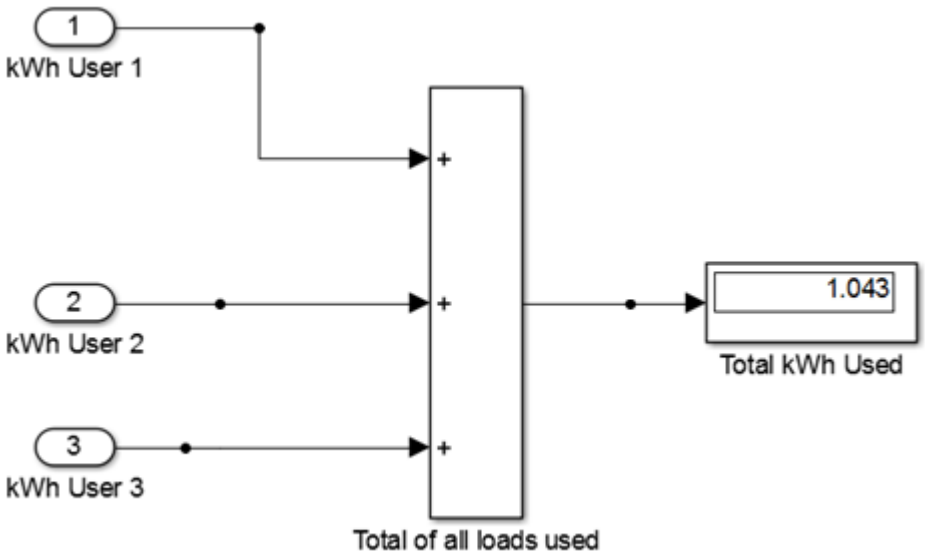

Figure 5.24: Summation of total load consumption

At the close of day, the ‘kWh User 1’ load value is taken and divided by the total user load consumption value as shown in the display, 'Total kWh Used' in Figure 5.24. This result is subtracted from one; the answer is divided by a value equal to the number of users less one. The resulting fraction is then multiplied by the battery reserve from Equation 5.2 to yield the energy allocation for 'User 1' from the accumulated reserve.

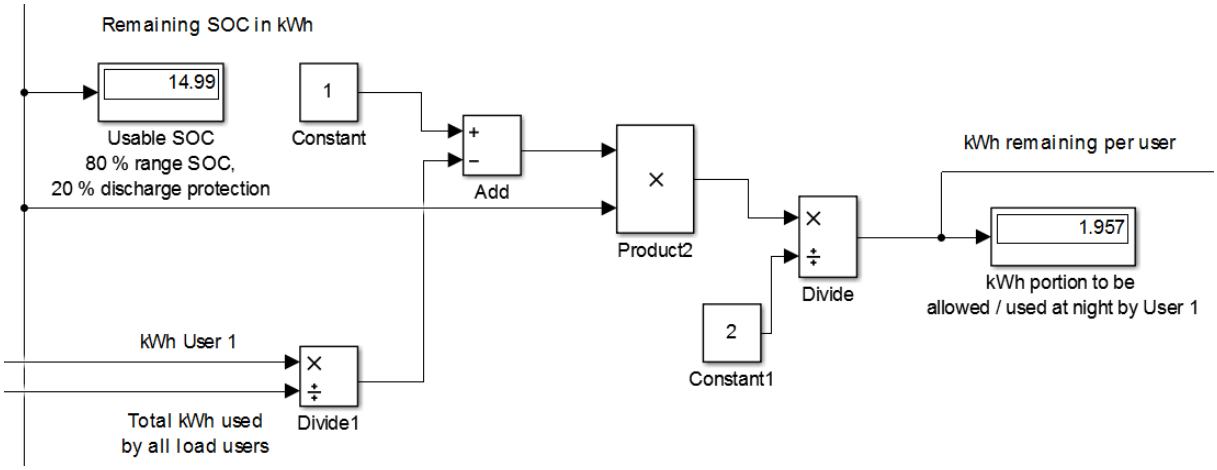

Figure 5.25: Remaining reserve share calculation

'N-users' indicates the number of users on the grid. 'Constant 1' is obtained by taking the number of grid users and subtracting one. In this test model a user count of three was selected and a value of '2' was inserted for 'Constant 1'; see Figure 5.25.

$$E_{available\ for\ User\ x} = \left[\frac{1-\left(\frac{E_{User\ x}}{E_{Total\ Users}}\right)}{[N_{Users}-1\,]}\right] \times E_{Battery\ Reserve} \tag{5.3}$$

5.13.4. Logic lock and control

The answer derived by Equation 5.3, namely the allocated energy (kWh), is passed to the input port of the 'Discrete Sample & Hold' block.

"Discrete Sample & Hold' will be active as long as the time of day is earlier than 18:00. Figure 5.26 depicts the hold block functions.

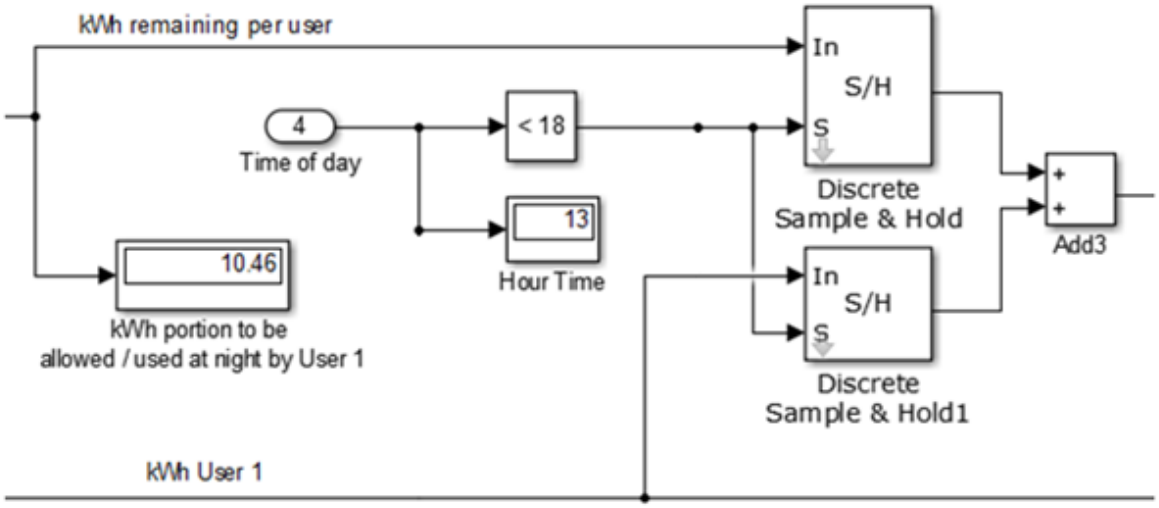

Figure 5.26: Hold and release power control logic

'Discrete Sample & Hold1' receives the value of a active user load during the day. This value is also retained when time of day is earlier than 18:00. The hold blocks are used to cumulatively add all the electrical energy drawn and to save the energy values when loads go on and off, as set by the Matlab user. If hold blocks are not used, then the maximum consumption value will not be saved. This is an important function in order for the next step to take place.

Values from both these hold blocks are added together by the 'Add 3' block and passed to the 'Add 4' block as shown in Figure 5.27. The user load consumption signal is connected to

the negative terminal of the ‘Add 4’ block. The added hold signals are connected to the positive terminal on the ‘Add 4’ block.

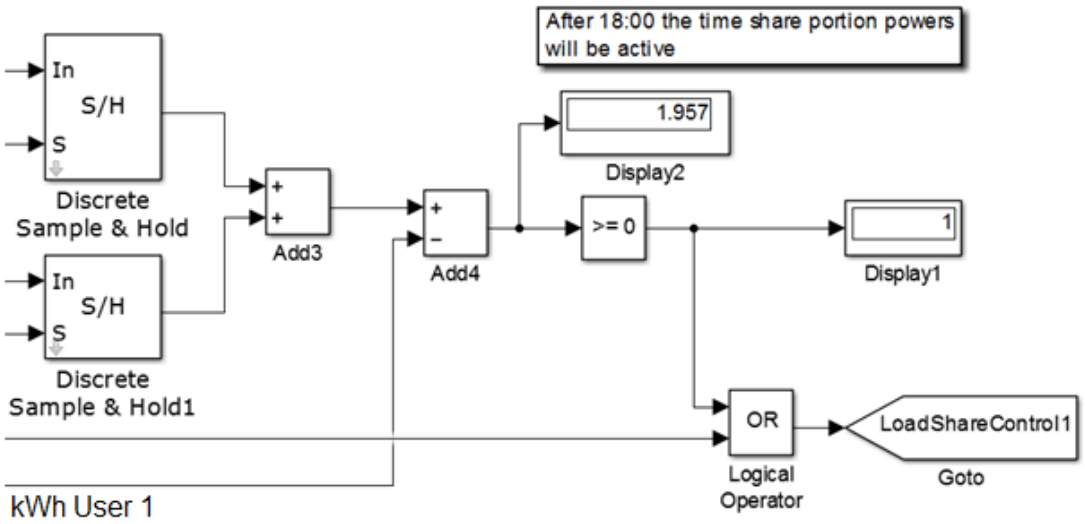

Figure 5.27: Load control from reserve share portion powers

Whenever the answer to the ‘Display 2’ block is above a zero value, then ‘LoadShareControl1’, shown in Figure 5.27, will be active. If the computed value is zero or smaller, then load shedding will be done via the ‘LoadShareControl1 link. ‘LoadShareControl1’ is linked to the ‘Load 1 Control’ subsystem via the ‘GoTo’ function. The function block will receive the enable/disable signal to manipulate the load according to the reserve share capacity. Figure 5.28 shows the simulation control flow chart. All the subsystems combined in this chapter are interlinked to form the process flow as indicated.

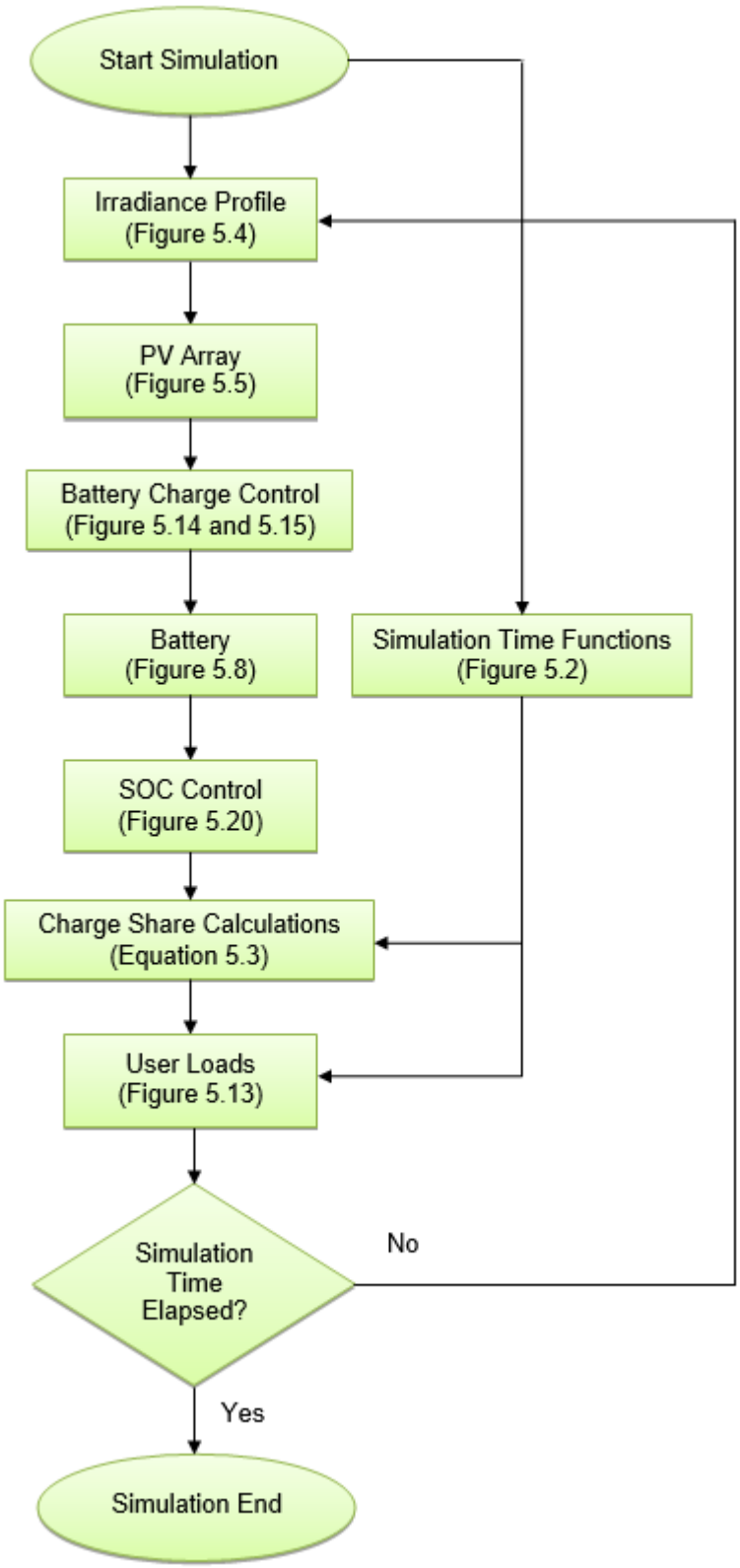

Figure 5.28: Simulation control flow chart

5.14. Hardware and software system

Simulation processing speed is dependent on the hardware computer system used for development and testing. This system was developed on Matlab version R2014a and testing was carried out on a computer hardware system with the following specifications:

- Windows 8 Professional, 64 Bit
- Central Processing Unit (CPU), Quad core, Intel, 2.67 GHz processors
- Memory, 8 GB memory

The real time for the model to run through a full simulation day takes between 7–9 minutes to execute. Processing speed is also very dependant on the number of display blocks used and the number of scope blocks connected to the simulator.

6. SIMULATION SETUP AND TEST SCENARIOS

6.1. MAS model setup

The Matlab user must do a model setup on the model subsystems before a simulation can be executed. The model will react to the parameters fed into the program at setup time. The following parameter functions will be explained and should be adjusted prior to simulation runs:

- Irradiance profile
- Boost constant
- Battery size and capacity
- Charge share calculations and battery referencing
- User load profiles
- Load under SOC load shed control
- Battery charge control limits

6.2. Irradiance profile

Battery charging and load energy is provided from the PV sources. The irradiance reference profile sets the base level isolation exposure of the these PV panels. Variations from this reference profile would create simulations of higher or lower irradiation intensity over longer or shorter days to simulate seasons, and cloudy weather. If low irradiance profiles are adjusted to, then the batteries might not get sufficient charge to increase the SOC to a sufficiently high level. The charge share logic will start execution from 18:00 time, in order to carry out the share logic. The x-axis in Figure 5.4 represents 86400 seconds to show the total number of seconds for a 24 hour day. The y-axis in Figure 5.4 represents the irradiance level from the sun onto the surface area of the PV panel, with the rays of the sun perpendicular to the panel surface.

6.3. Boost constant

A boost constant can be inserted into the ‘'Current Source Boost Constant Subsystem’ block (see Figure 5.1); by selecting a suitable boost constant, one can effectively increase the irradiation and thereby also increase the power output of the PV source. If the boost value is not used, then multiple PV panels will have to be programmed in parallel, to provide more current for the charge loop whilst keeping the bus voltage constant in a particular configuration. When the boost value is kept to a value of one, the reference current as determined by the reference irradiation profile, will be generated. When a bigger value, like

five for example, is used as a boost value, the current generated by PV panel will be five times bigger than the reference current. Charging of the batteries will be more rapid with a higher boost value and the SOC gradient will be steeper than when a boost value of one is used. Where a boost value resulting in the simulation of multiple panels is used, the resulting panels act as if they are connected in parallel. For example for a boost value of 45, the model will simulate the output of 45 panels in parallel.

6.4. Battery size and capacity

The charge share logic system requires the battery capacity and SOC to calculate the different amounts of stored energy available to each user overnight.

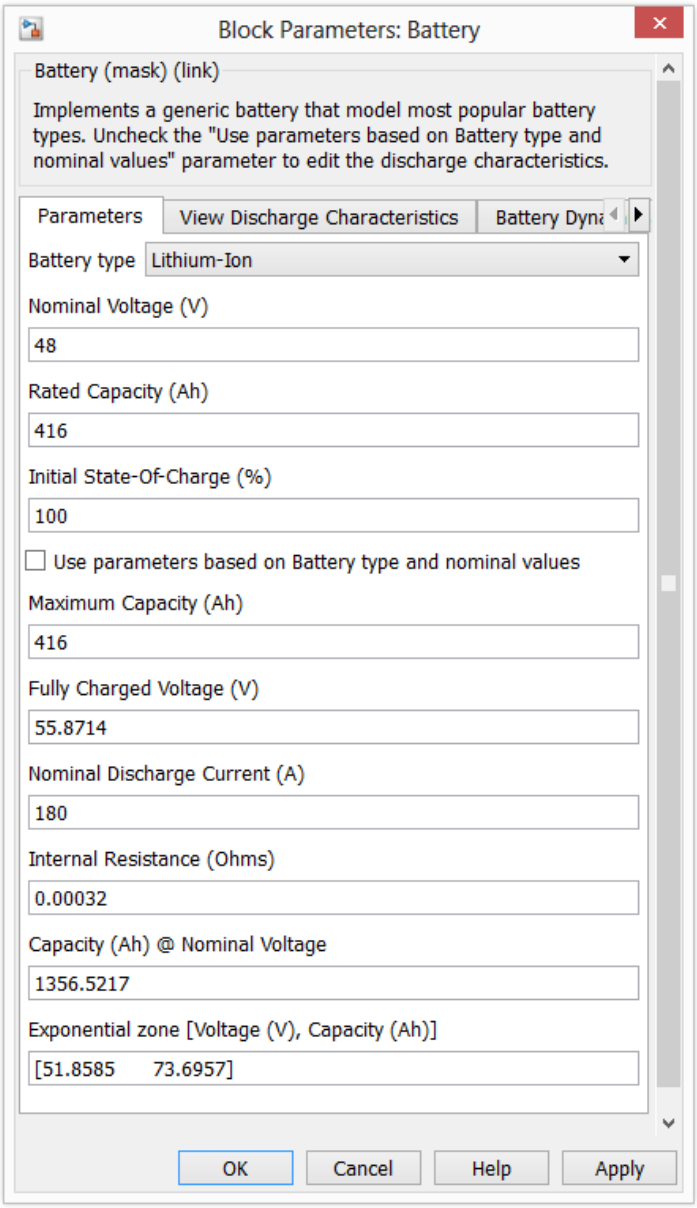

Figure 6.1: Battery block parameters

Open the 'Battery' block as shown in Figure 6.1, to enter the battery settings. It is only required to enter the nominal voltage value, rated battery capacity and the initial state-of-charge. This study will keep the bus voltage at 48 V DC.

The 'Initial State-Of-Charge' entered gives the charge of the battery at the start of the simulation, compared to a fully-charged battery. Note that the battery charge control is set up to protect the battery from total discharge. Thus the battery will be charged to an SOC of 60% before load consumption is allowed, when the battery was previously drained to a SOC of 20%. If the Matlab user wants a user in the simulation to consume power from the batteries from 00:00 to 12:00, then note should be taken to set the SOC to a higher value than the SOC limit to run morning loads; this implies that the loads are run off the battery.

6.5. Charge share calculations battery referencing

It is critical that the values inserted into the battery set points for 'Nominal Battery Voltage' and 'Capacity in Ah', as shown in Figure 6.1, are copied exactly from the corresponding values used in Figure 6.2. The whole range of scaling calculations for the battery charge share concept, use these parameters.

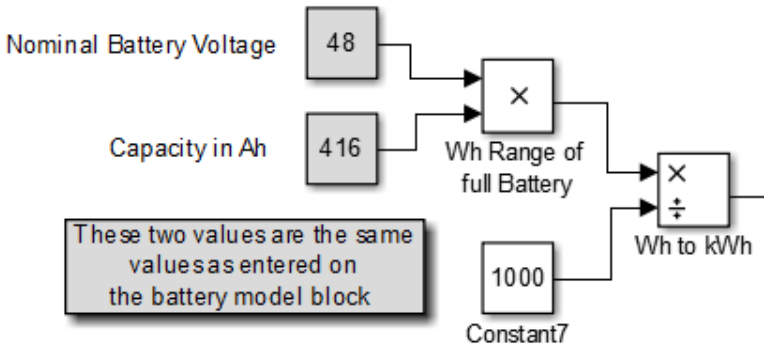

Figure 6.2: Battery set points inside charge share calculations referencing subsystem

6.6. User load profiles

The user load profile arrangement is adjusted for the energy demanded by the user from each house. Load shedding is implemented by an algorithm which determines when to switch a particular house unit onto or off the grid. All the different agent subsystems calculate processes and execute logic controls that respond to the environment and deal with user load shedding.

Within the ‘Load Control’ subsystem the Matlab user selects the RLC component by entering its adjustable parameters. The active power parameter in Figure 6.3 is adjusted to provide the load that a house unit will draw. The next RLC component can be selected to add more

loads that are switched into the circuit during their scheduled time settings. From the daily loads and their time slots, the energy demand profile of a particular house can be determined. This will give load changes within a house load profile. If more switching patterns are desired, then more RLC components can be inserted.

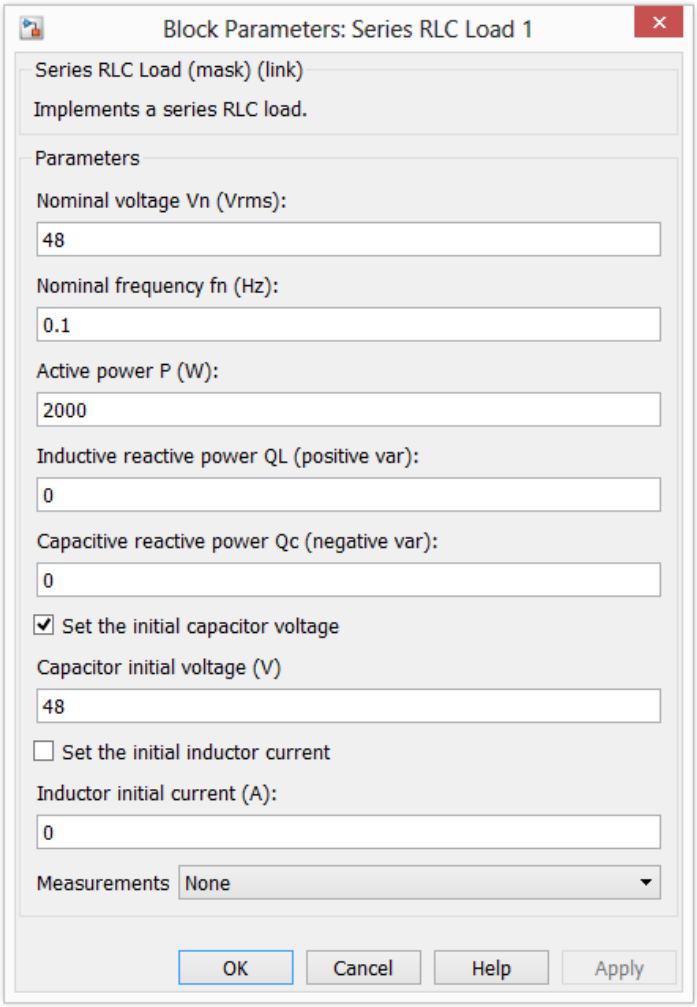

Figure 6.3: Series RLC block parameters

'Interval Test' blocks as shown in Figure 5.13 are connected to the ‘Hour_of_day’ block. Select the 'Interval' blocks and adjust the number of hours the respective loads will be on.

The load profile is decided before the model is started and is a fixed setup for the whole simulation day. The charge share algorithm will adjust the load shedding according to the consumer energy ratings, the bus voltage status and the SOC of the battery. When the model goes into charge share mode, it will manipulate the excess of the amount of energy that is left to a particular user. The above-mentioned profile will consume energy from the available stored energy limit until it is depleted.

6.7. Load under SOC load shed control

Load shedding will be done to disconnect all the grid loads when the battery SOC is low; this function serves to protect the battery and prolong its life span. Figure 5.20 indicates the high and low SOC limits. The low limit in this example will open load connections to the grid when the SOC is 20%. At an SOC of 60% load users will be re-connected to the grid.

6.8. Battery charge control limits

The voltage bus control limits will regulate the bus voltage level between the two limits as defined by the Matlab user (see Figure 5.16). The SOC limit is set to allow the battery to charge when the limit has dropped below a predefined value. The high and low voltage parameters are also defined in Figure 5.16.

6.9. Test scenarios

A simulation platform for an agent-based microgrid has been designed. The above-mentioned parameters were set up to create unique daily operating scenarios by adjusting the power source and the energy requirements. Different load patterns, battery settings and irradiance profiles were selected beforehand, to provide the pre-setup for each scenario. The goal was to monitor how the charge share concept responds to load variations and to confirm that the correct percentage of battery SOC energy shares are divided between the load users. The objective was to establish that the allocation of the available stored energy among the users is executed by the algorithm. The pre-setup parameters of each scenario was selected as follows: for each scenario these parameters have been tabulated for easy reference.

The results of the simulated scenarios set out below, are presented in Chapter 7. The irradiance profile shown in Figure 5.4 is used as the irradiance reference. The bus voltage specification will remain on 48 V. The aim of this thesis is to derive a formula that will allow division of power between users, taking into account their individual consumption during the daytime; this was achieved in Chapter 5 with the derivation of Equation 5.3 with example of loads. At the end of the simulation, it is expected to see the energy values being calculated and where the inverse calculated values of consumption is allowed back to the users as divided from the remaining SOC. The cut-off time for when a day will come to its end regarding the absorption of energy from the sun, has been programmed to occur at 18:00. This is the time when the charge share logic will start to take control of the power management.

6.9.1. Scenario A

The first model, Scenario A, models a basic user profile. The irradiance boost constant was selected as 45 to simulate the incorporation of 45 PV panels for grid generation. A SOC of 100%, representing a fully charged battery, was selected, while a battery capacity rating of 2000 Ah was selected. To validate that the system mathematics are functional, the loads and durations were made the same for all three users. Each user used 1000 W continuous power for the full day. The expected result should reflect equal energy division between all users. Table 6.1 indicates the initial parameters for setup to Scenario A.

Table 6.1: Scenario A: model setup parameters

Irradiance profile	See Figure 5.4
Irradiance boost constant	45
Battery size and capacity	Voltage: 48 V DC Capacity: 2000 Ah Initial SOC: 100%
User 1 load-time reference	Load Size: 1000 W Consumer demand times: 24 hours
User 2 load-time reference	Load Size: 1000 W Consumer demand times: 24 hours
User 3 load-time reference	Load Size: 1000 W Consumer demand times: 24 hours
Load under SOC load shed control	SOC limit to reset and open disconnect all loads from the grid: 20% SOC limit to set and connect loads back to the grid: 60%
Battery charge control limits	Charge on: $V_{battery} < 48$ V and SOC < 70% Charge off: $V_{battery} > 55$ V

6.9.2. Scenario B

In Table 6.2 the setup for Scenario B is shown. The irradiance constant was set at 30 units to have a smaller charge effect on the grid than was the case for Scenario A. The initial SOC was set at 65% to monitor the discharge characteristics of the DC bus. Variable loads were introduced for User 1, while the load User 2 and User 3 was respectively set to a constant 1200 W and 1000 W. The aim was to inspect the control properties of the charge share calculations when the algorithm was introduced to variable load changes.

Table 6.2: Scenario B: model setup parameters

Irradiance profile	See Figure 5.4
Irradiance boost constant	30
Battery size and capacity	Voltage: 48 V DC Capacity: 2000 Ah Initial SOC: 65%
User 1 load-time reference	Load Size: 500 W + 800 W Consumer demand times for 800W: 04:00–07:00 12:00–13:00 17:00–23:00 Constant 500 W load for 24 hours
User 2 load-time reference	Load Size: 1200 W Consumer demand times: Morning: None Afternoon: None 18:00–24:00
User 3 load-time reference	Load Size: 1000 W Consumer demand times: 04:00–07:00 17:00–23:00
Load under SOC load shed control	SOC limit to reset and open disconnect all loads from the grid: 20% SOC limit to set and connect loads back to the grid: 60%
Battery charge control limits	Charge on: $V_{battery} < 48$ V and SOC < 70% Charge off: $V_{battery} > 55$ V

6.9.3. Scenario C

Below in Table 6.3, the setup to Scenario C is given, where the irradiance boost value was set at 10 units. This number of PV panels will provide a smaller amount of charging effort than was the case for Scenario B; this reduced array was selected to monitor how the grid would function with a reduced energy input. The battery capacity was set at 1000 Ah and initial SOC was set at 60%. The charge share algorithm was monitored during the energy share calculation processes and the effect of load crossing on the algorithm was observed. Load crossing is the situation when two or more user load graphs cross. The aim was to observe the allocation of energy while the user consumption varies.

Table 6.3: Scenario C: model setup parameters

Irradiance profile	See Figure 5.4
Irradiance boost constant	10
Battery size and capacity	Voltage: 48 V DC Capacity: 1000 Ah Initial SOC: 60%
User 1 load-time reference	Load Size: 300 W + 1000 W Consumer demand times for 1000 W: 04:00–07:00 12:00–13:00 17:00–23:00 Constant 300 W load for 24 hours
User 2 load-time reference	Load Size: 2000 W Consumer demand times: 11:00–13:00 16:00–24:00
User 3 load-time reference	Load Size: 1500 W Consumer demand times: 06:00–08:00 12:00–13:00 17:00–22:00
Load under SOC load shed control	SOC limit to reset and open disconnect all loads from the grid: 20% SOC limit to set and connect loads back to the grid: 60%
Battery charge control limits	Charge on: $V_{battery} < 48$ V Charge off: $V_{battery} > 55$ V

6.9.4. Scenario D

Scenario D is presented in Table 6.4 where the initial SOC was set at 45%. The number of PV panels is 35 and the battery capacity is 1500 Ah. The variable load values were increased to subject the grid to a higher load. The aim was to monitor how the battery SOC varied with bigger loads, as compared to those of Scenario C. The SOC protection function was monitored to show how it reacts to SOC limits. The charge share algorithm was monitored during the energy share calculation processes and to see how load crossing affects the algorithm.

Table 6.4: Scenario D: model setup parameters

Irradiance profile	See Figure 5.4
Irradiance boost constant	35
Battery size and capacity	Voltage: 48 V DC Capacity: 1500 Ah Initial SOC: 45%
User 1 load-time reference	Load Size: 1500 W + 500 W Consumer demand times for 1500 W: 04:00–07:00 12:00–13:00 17:00–23:00 Consumer demand times for 500 W: 14:00–17:00, 20:00–24:00
User 2 load-time reference	Load Size: 1300 W Consumer demand times: 05:00–08:00 11:00–13:00 16:00–24:00
User 3 load-time reference	Load Size: 3000 W Consumer demand times: 06:00–08:00 12:00–13:00 17:00–24:00
Load under SOC load shed control	SOC limit to reset and open disconnect all loads from the grid: 20%, SOC limit to set and connect loads back to the grid: 60%
Battery charge control limits	Charge on: $V_{battery} < 48$ V Charge off: $V_{battery} > 55$ V

7. SIMULATION RESULTS

7.1. Expected results

Each grid user had a pre-defined daily load pattern; all user load and their durations were recorded. If a load user used a small amount of energy during the daytime, then a large part of the available stored energy needs to be allocated to that user. If a user consumed a large quantity of energy during the daytime, then, if working correctly, the algorithm should only allocate a small amount of available stored energy during the night up to 24:00. All three user energy totals are used to calculate the charge share energy capacities to be allocated accordingly at 18:00. All energy allocated to each user by the algorithm, must, upon execution be displayed on suitable graphs. System parameters are adjusted to take account of external factors so that the effect of these external factors (weather, load patterns) are taken into account when the model is run.

7.2. Simulation result monitoring and recording

Measurement of parameters was done with ‘Scope’ blocks. ‘Display’ blocks are used to display values within the Matlab program. In the subsections of this section, feedback obtained from simulation runs of the model caused changes in specific variables; data relating to these variables was monitored and recorded.

7.2.1. Load consumptions

The cumulative energy consumption of each of the three grid users over the day, was plotted to provide a visual representation of their respective energy use patterns.

7.2.2. SOC, battery voltage and battery current

The battery SOC, battery voltage and battery current were monitored to illustrate bus voltage fluctuations, the charge level of the battery and the charge–discharge current of the battery.

7.2.3. Charge share calculation energy values

These are the energy values to be allocated to each user when the charge share logic is enabled at 18:00; the cumulative totals of each of the users at this time are of particular interest. Each user’s energy share value is calculated and adjusted taking account of the cumulative energy consumed by the user in relation to the total cumulative energy output at the cut-off time.

7.2.4. Confirmation of charge share values on an Excel spreadsheet

The Matlab model algorithm calculates the available energy portion of the battery SOC at 18:00. Equation 5.3 is the reserve share formula that has been used in Microsoft Excel to set up in a spreadsheet to show what the energy allocation should be for a given SOC. The charge share calculation results in Matlab should compare to the spreadsheet results at 18:00.

7.3. Results and discussion of the graphs

This section contains all the graphs and data recordings taken from the Matlab model scope measuring blocks.

7.3.1. Scenario A: results and discussion

The input setup prior to the simulation run for Scenario A was given in Chapter 6. In Figure 7.1 it shows that the battery SOC was 100% at the start of the simulation. The user loads were set up to be the same for this test and drew a combined total current of 60 A. The battery voltage started at 56 V and reduced by 2 V when the load started to consume battery energy. For this scenario the user loads were set up to draw power continuously throughout the 24 hours of the simulation. A gradual decline in the SOC was noted from 00:00 until 08:48 when SOC reached the 70% limit for charging. Charging parameters were set up to start charging at 70%. Battery current dropped to negative 180 A when battery charging was initiated. The SOC increased to 100% from 08:48–11:54 due to charging. The battery voltage increased back to 55 V when the battery had been charged to 100%.

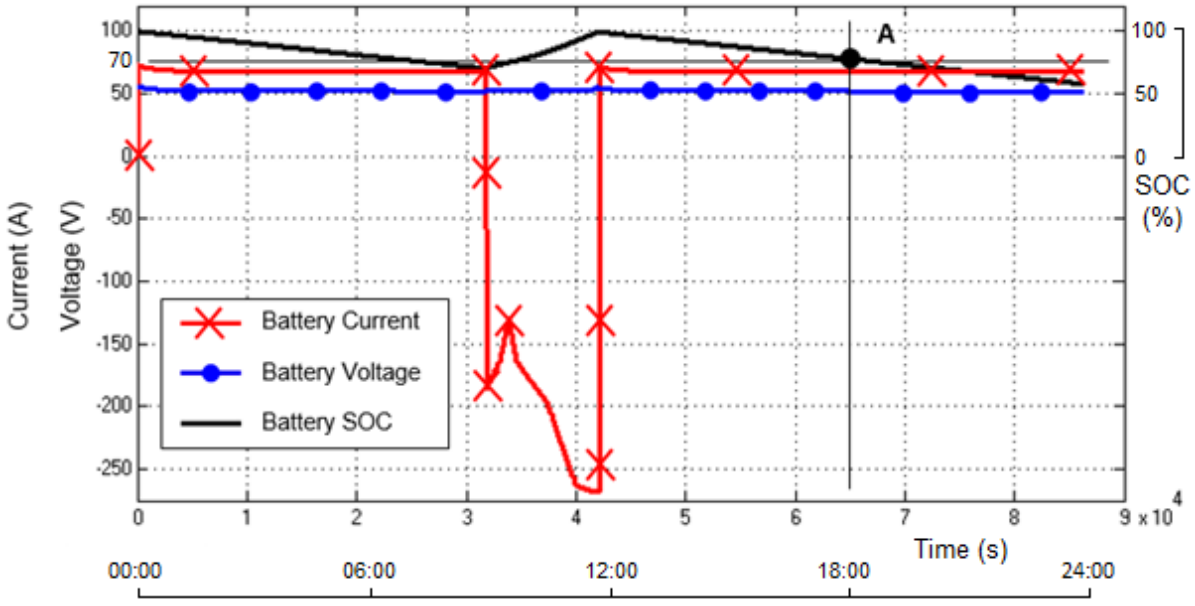

Figure 7.1: Scenario A: battery status

Battery charging stopped at 100% SOC level at 12:00. In Figure 7.2 it can be seen that the user load consumption rose at the moment when charging stopped, due to the rise in the bus voltage when the battery SOC reached 100%. As shown in Figure 7.1 the battery SOC decreased gradually after 12:00; a 2-3 V drop is noted when the SOC is decreased due to user energy consumption. Point A represents the point when the reserve share logic is activated in the simulation model. Without any sun, no charging is possible after 18:00; load control is activated beyond this time. Point B in Figure 7.2 shows what all the load consumptions were for the day at 18:00. All user loads were confirmed to have consumed the same power with all three consumption graphs tracking on top of each other. Point B also indicates that all users had consumed 21 kWh from 00:00 until 18:00. Charge reserve share energy was continuously calculated and reflected as shown in Figure 7.3.

Equation 5.3 was used to calculate the percentages of electrical energy that were allowed at the given battery SOC. The full battery at start-up time, 00:00, held 76 kWh of usable energy which represented 80% of its SOC. Each user was allocated a third of this starting total, which was 25.3 kWh. The energy values that were allocated to each user were the same because the energy consumption of each user during the day, from 00:00 to 18:00 was identical; hence the trend lines as shown in Figure 7.3, run on top of each other.

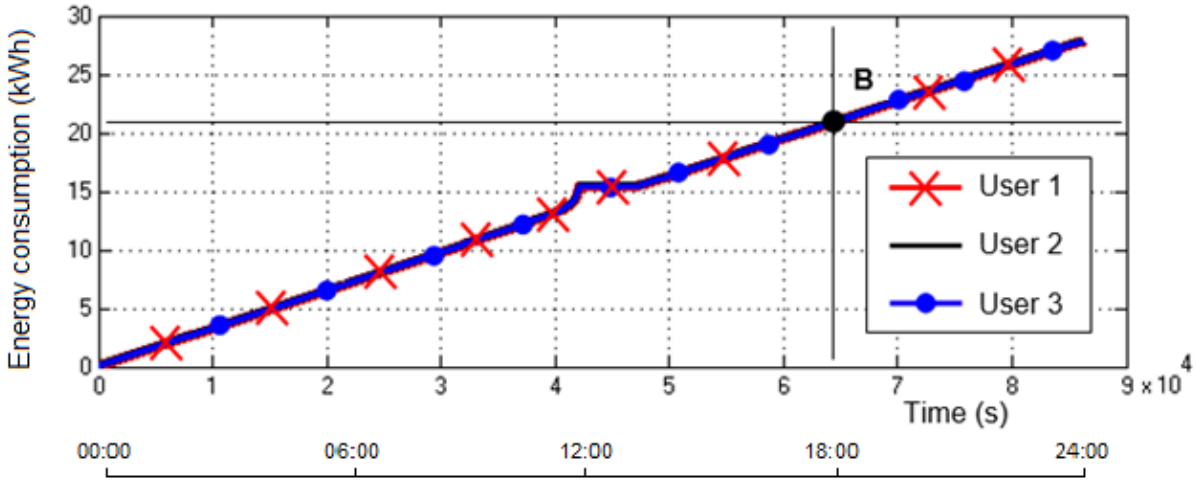

Figure 7.2: Scenario A: energy consumption

If the change in energy allocation in Figure 7.3 is compared to the battery SOC in Figure 7.1, it will be observed that the change in allocation of energy to each of the three users, was directly related to the change in battery SOC. Point C at 18:00 in Figure 7.3 shows the point at which the reserve share logic was activated.

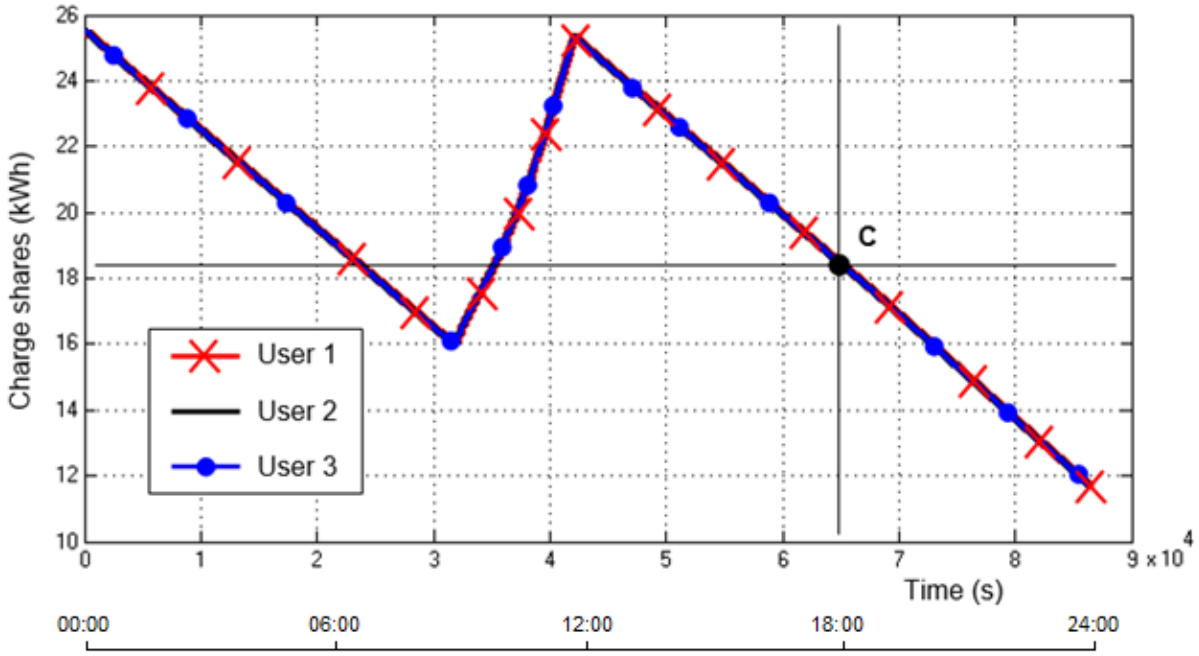

Figure 7.3: Scenario A: energy allocation

As shown in Figure 7.3, each user unit was allowed a 19.3 kWh energy portion from the remaining battery SOC at 18:00. Table 7.1 presents a summary of user values for this test. Equation 5.3 was used in the Excel spreadsheet to validate the test points against the graphic result.

Usable battery energy of 76 kWh is calculated where 20% SOC was subtracted from the full battery range of 96 kWh. The algorithm divided the reserve share energy, equally between the three users, each receiving a 33.3 % energy share. This test confirmed that the reserve share logic and formula is functional with equal results of charge share when equal load consumption values were presented. Table 7.1 gives a summary of the charge share persentage values at 18:00 and the allocation of energy between the users.

Table 7.1: Scenario A: result summary

Simulator graph variables	Value
Measured usable battery energy at 18:00 (kWh)	58
Full battery Energy (kWh)	76
Battery SOC (%)	76.32
Calculated energy level left in battery (kWh)	58

	Results		
User no.	Energy consumption 00:00 - 18:00 by each user (kWh)	Energy left for each load to use after 18:00	
		(kWh)	(%)
1	21	19.33	33.33
2	21	19.33	33.33
3	21	19.33	33.33
Total	63	58.00	100

7.3.2. Scenario B: results and discussion

In Scenario B, variable load changes were introduced to the system and the energy consumption changed to accommodate as shown in Table 6.2. The following parameters apply to this set up:

- The SOC limit protection was set to disconnect User loads on 20% and enable load control on 60%.
- The battery charge control limits were set at 48 V and 55 V.
- Charging of the battery was set to trigger when the SOC dropped to 70%.

As can be seen in Figure 7.4, the battery SOC started to perform on the pre-set value of 65% and reaches 100 % at 12:00. When charging starts at 04:15, the current declines from a value of +50 A to a value of -220 A at 12:00 when charging stops. Positive battery current spikes in Figure 7.4 at 04:15, 12:00, 17:00 and 18:00 shows where User loads were applied to the system. Negative battery current shows that the system was charging from 04:15–12:00. The negative spikes at 13:00 and 23:00 indicates where user loads have been disconnected from the system. The negative spike at 21:30 indicates where User 1 was disconnected when the user's remaining energy portion was depleted before the end of the day.

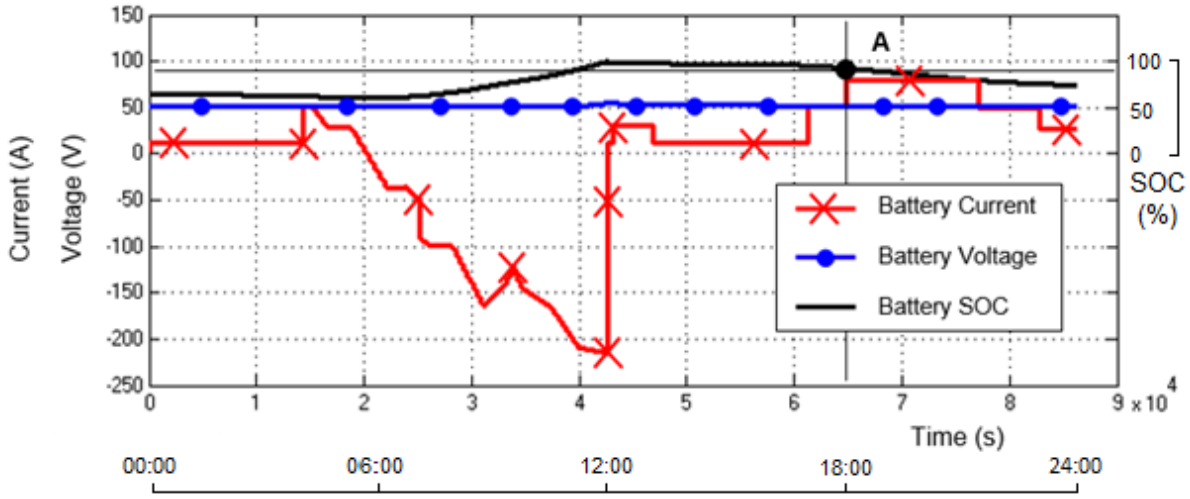

Figure 7.4: Scenario B: battery status

At Point A in Figure 7.4, the battery SOC is 90% at 18:00. Points B, D and C in Figure 7.5 show the respective cumulative energy consumption for each user at this time. User 1 has two constant loads, 500 W and 800 W respectively. The 800 W load is demanded intermittently and the 500 W load is required for the full 24-hour period. User 2 starts to consume energy at 18:00. User 3 consumed energy once in the morning at 04:00 and then again at 18:00.

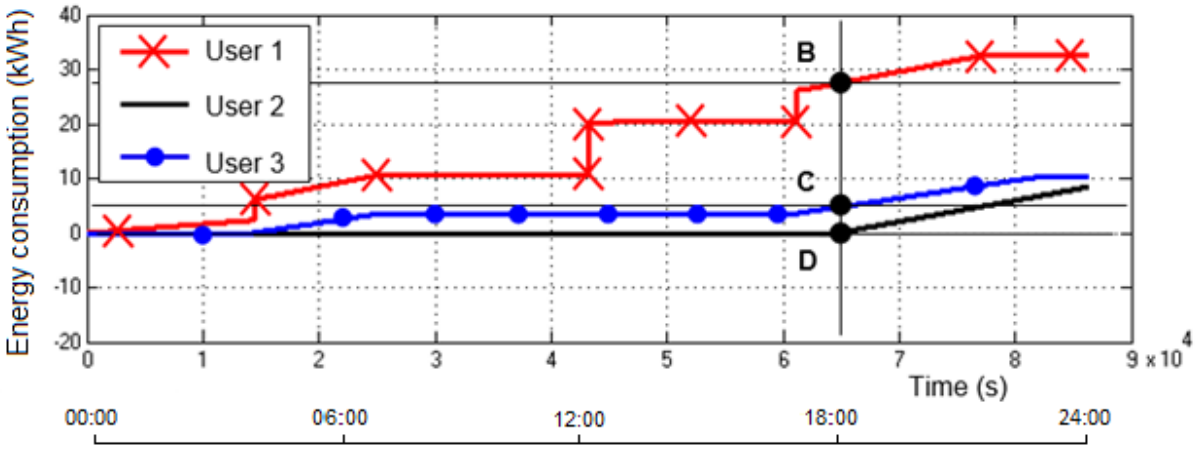

Figure 7.5: Scenario B: energy consumption

Figure 7.6 indicates the charge values calculated throughout the day using Equation 5.3. As can be seen in Figure 7.5, User 1 at Point B was the biggest energy user. If we look at the red line that indicates User 1 in Figure 7.6 then it is evident that the charge share algorithm allowed the least amount of stored energy to this user. In the case of Users 2 and 3 where we see that they were allowed the same charge up until 04:15.

Points G, E and F show the respective charge share values for Users 1, 2 and 3 at 18:00. At 18:00, the charge share algorithm stopped calculating the charge energy portions and only allowed the remaining portion energies to be deducted. This may explain why all the trend lines show a declining slope from 18:00 onwards.

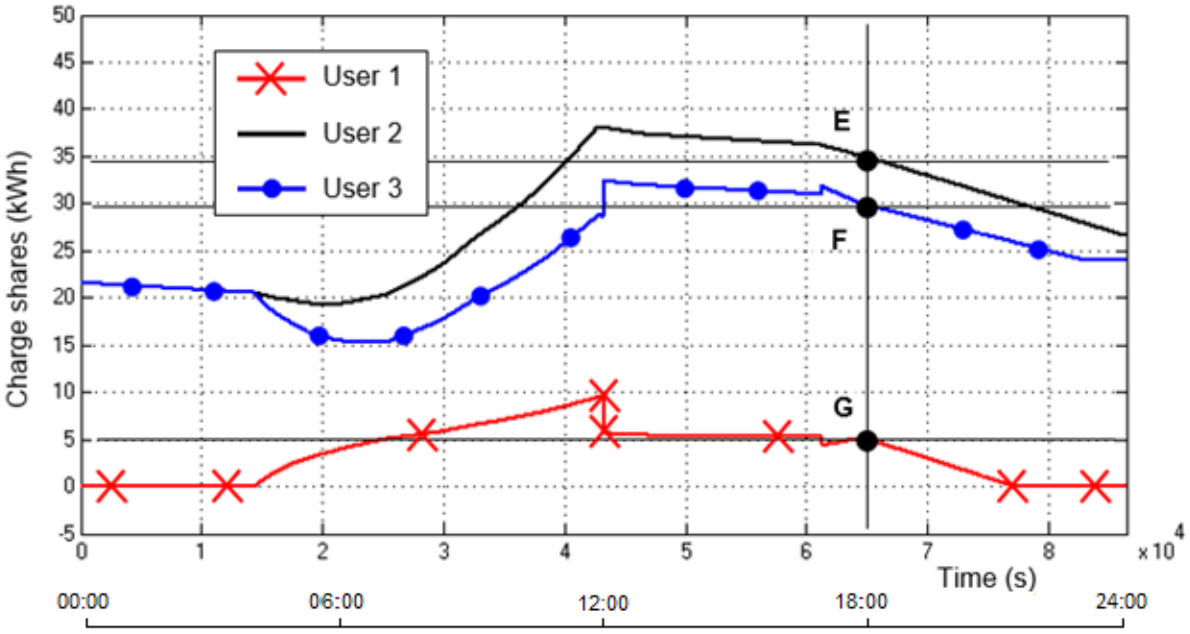

Figure 7.6: Scenario B: charge share

The lines show decreasing charge stress values when the loads are still consuming energy after 18:00 and will change to horizontal lines when the loads are switched off inside the houses.

Table 7.2: Scenario B: result summary

Simulator graph variables	Value
Measured usable battery energy at 18:00 (kWh)	68.40
Full battery Energy (kWh)	76.00
Battery SOC (%)	90.00
Calculated energy level left in battery (kWh)	68.40

	Results		
User no.	Energy consumption 00:00 - 18:00 by each user (kWh)	Energy left for each load to use after 18:00	
		(kWh)	(%)
1	28.00	5.15	7.58
2	0.00	34.00	50
3	5.00	28.85	42.42
Total	33.00	68.00	100

Table 7.2 is extracted from Microsoft Excel to verify the load sharing percentages. It is positively identified that User 1 used the most energy during the day and was allowed the

smallest portion of battery SOC at 18:00. User 2 was allowed 50% of the remaining charge because no power was consumed during the day. User 3 received 42.42% of the remaining SOC and was recorded as the medium user for the day with a consumption of 5 kWh before 18:00.

This test proves the functionality of the charge share algorithm with variable load profiles operating on the microgrid. The biggest user of the day was allowed the smallest portion of remaining SOC energy at night, whereas the smallest power user was allowed the biggest share of available energy at night.

7.3.3. Scenario C: results and discussion

Scenario C also has variable loads but with fewer PV panels — see Table 6.3. The goal of this test was to see how Equation 5.3 would deal with energy division when user graphs crossed, as can be seen in Figure 7.8.

Figure 7.7 shows that the battery SOC was 60% at 00:00. The limit was set to allow load coupling when the value of SOC is greater than 60%. The moment when the sun started to rise at 04:00 as taken from Figure 5.4, charging occurred as can be seen in the variation of battery current. This eventually increased the SOC above the limit where grid loads are coupled back onto the grid.

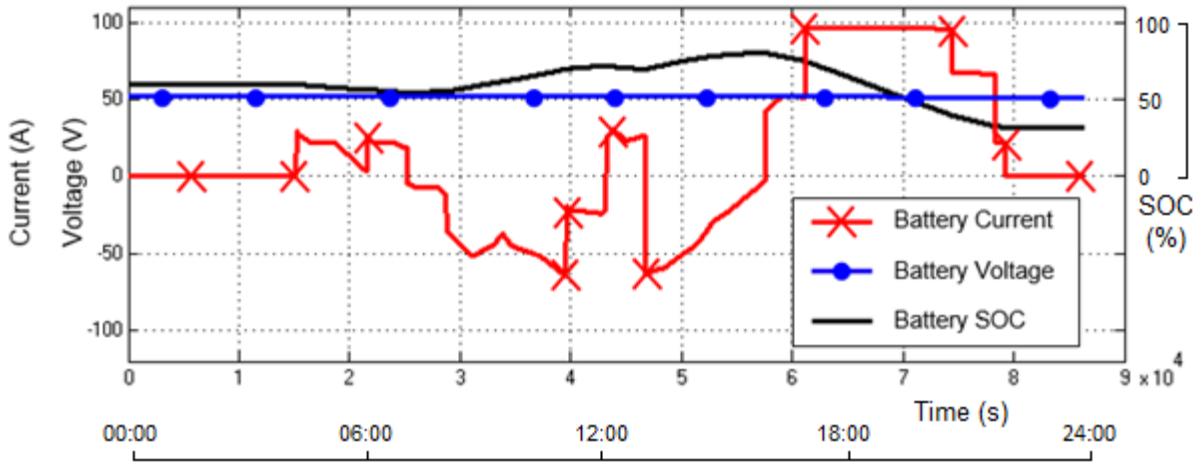

Figure 7.7: Scenario C: battery status

The load of User 1 was on at 04:00, as shown in Figure 7.8. For User 1 the model was set up for a constant load of 300 W over 24 hours; energy consumption is not visible from 00:00–04:00 because the SOC protection limit of 60% was not reached yet. User 3 starts to draw energy from the grid at 06:00 while User 2 only starts at 11:00.

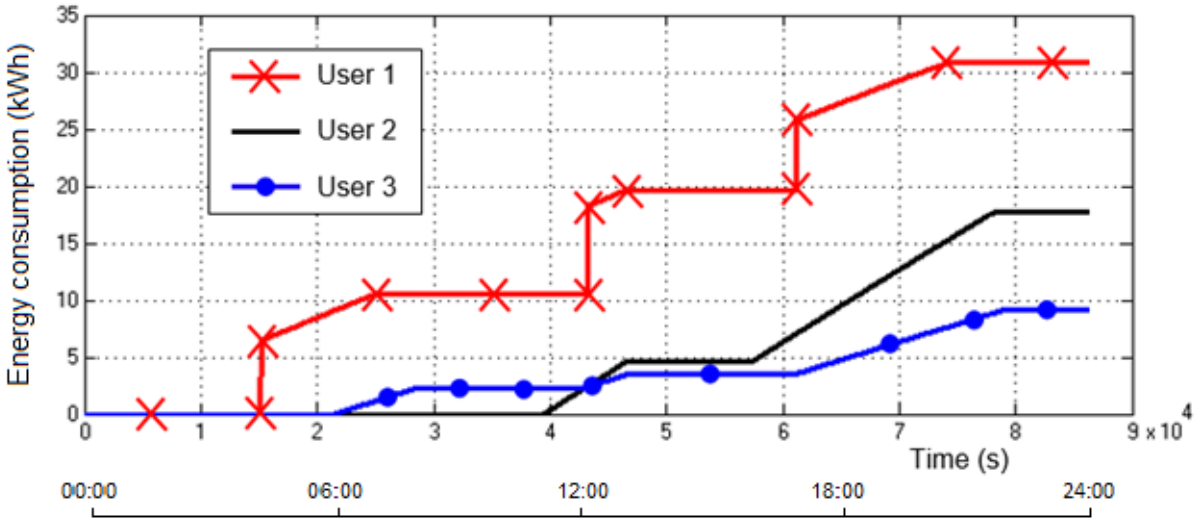

Figure 7.8: Scenario C: energy consumption

At 12:30 the cumulative energy used by User 2 exceeded the cumulative energy used by User 3.

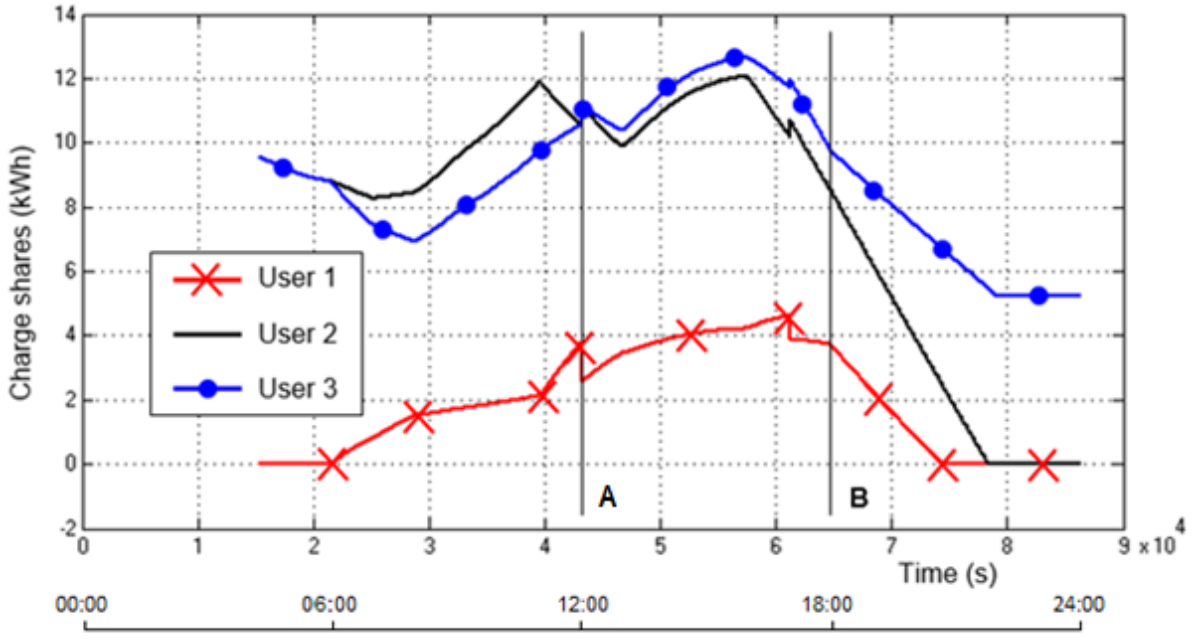

Figure 7.9: Scenario C: charge share

Figure 7.9 shows the effect of load crossing on the charge shares as indicated by line A which corresponds with the load crossing time of 12:30 shown in Figure 7.8. Note that the graphs only started to record from the 04:00 as processing of the charge share recording will only occur when any one of the loads starts to draw energy from the grid.

Line B indicates the time at 18:00 when the reserve share logic takes over in the program. Consumption lines will only have negative gradients from line B onwards, until the 24:00 is

reached. Users 1 and 2 deplete their energy charge share at 19:30 and 21:30 respectively. User 3 was cut off at 22:00 at which time the consumption was 5.2 kWh.

This test confirmed that the Matlab program successfully execute the output from Equation 5.3 during load crossing. A summary of the results of this test are given in Table 7.3.

Table 7.3: Scenario C: result summary

Simulator graph variables	Value
Measured usable battery energy at 18:00 (kWh)	23.40
Full battery Energy (kWh)	38.40
Battery SOC (%)	60.00
Calculated energy level left in battery (kWh)	23.04

	Results		
User no.	**Energy consumption 00:00 - 18:00 by each user (kWh)**	**Energy left for each load to use after 18:00**	
		(kWh)	**(%)**
1	27.50	3.72	15.88
2	8.00	9.38	40.07
3	4.80	10.31	44.04
Total	40.30	23.40	100

7.3.4. Scenario D: results and discussion

The variable load values in this scenario were increased to subject the grid to a higher load as outlined in Table 6.4. This was done to test how the battery SOC varies with larger loads than were used in Scenario C. The battery SOC was set to 45% for this simulation, with an operating limit of 60%. Figure 7.10 and Figure 7.11 show the battery status and user energy consumption respectively, for 24 hours.

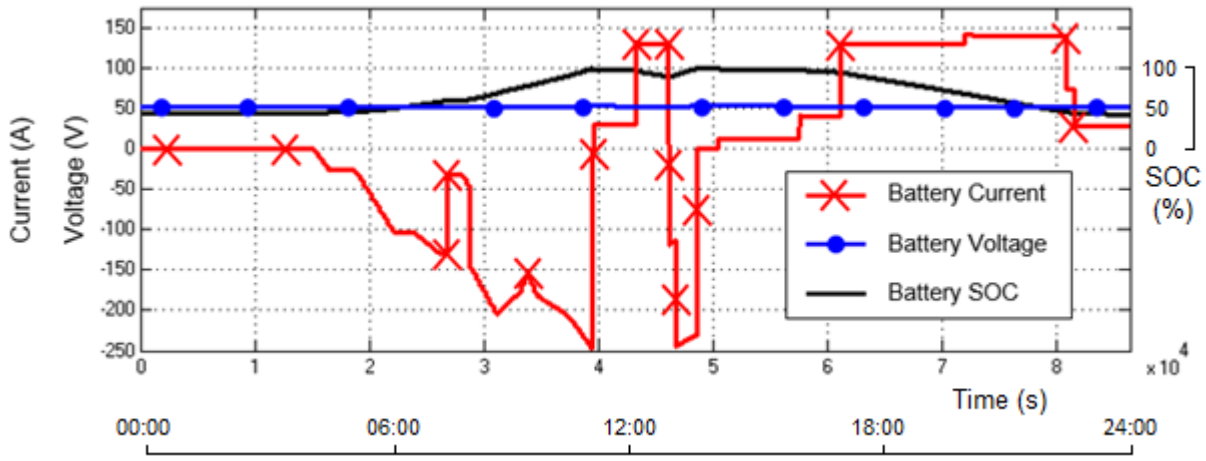

Figure 7.10: Scenario D: battery status

Users only started to consume energy at 07:30 when the SOC reached 60% and charging stopped at 11:00 when the SOC was 100%. Charging was initiated again at 13:30 for half an hour, but did not occur again before 24:00; this is due to the fact that the voltage level remained above 48 V. The steps after 14:00 for the battery current show where loads were applied and disconnected. Energy consumption started to occur at 07:30 in Figure 7.11. All the steps in Figure 7.11 shows where loads have been switched on. Positive gradient lines show the moment when users consumed energy and horizontal lines indicate where no energy was consumed.

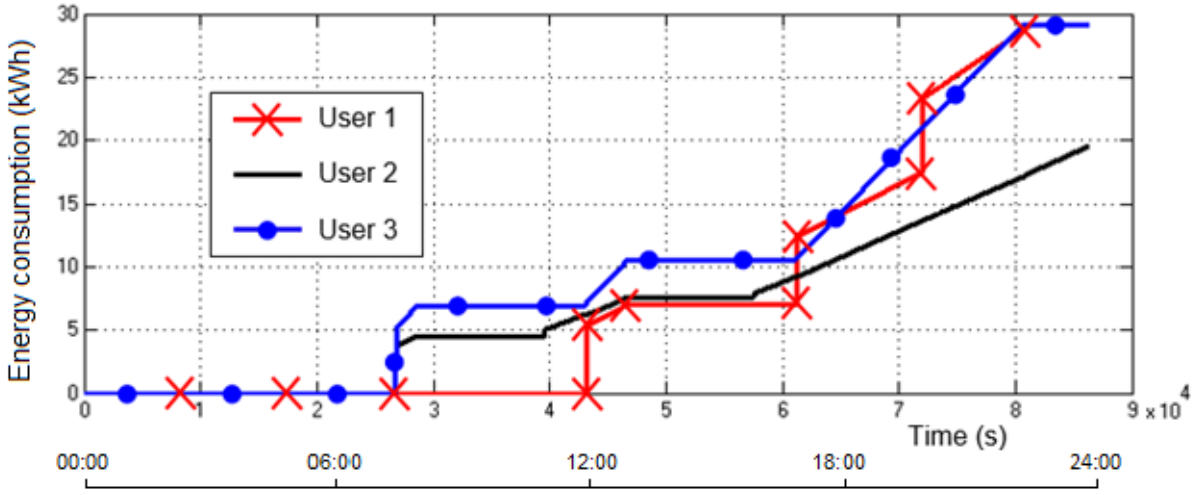

Figure 7.11: Scenario D: energy consumption

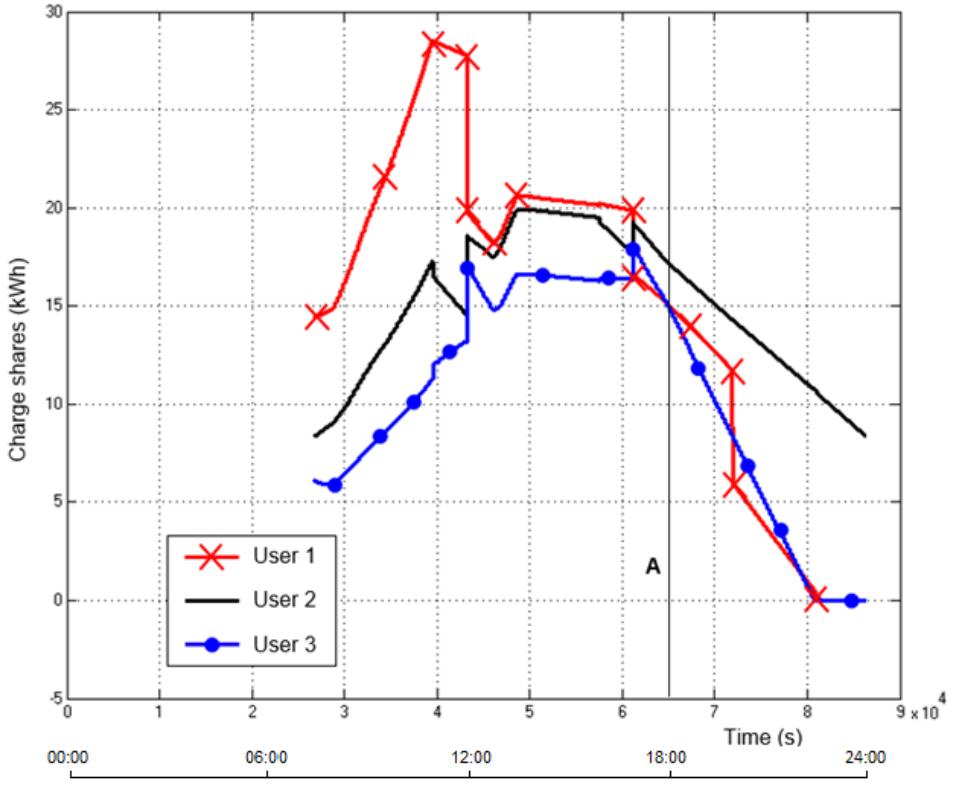

Figure 7.12: Scenario D: charge share

The SOC is 80% at 18:00 at A in Figure 7.10. User 1 and User 3 have consumed the same amount of energy at A and so were also allocated the same amounts of the available stored energy in the batteries.

User 2 consumed the least amount of energy during daytime. This allows User 2 to consume a bigger portion of energy available after 18:00 than the other users. At around 22:15 in Figure 7.12, both Users 1 and 3 was de-coupled from the grid as their charge share energies had been depleted. User 2 still continued consuming energy until 24:00.

Scenario D indicates that the simulation can successfully handle larger loads.

Table 7.4: Scenario D: result summary

Simulator graph variables	Value
Measured usable battery energy at 18:00 (kWh)	46.08
Full battery Energy (kWh)	57.60
Battery SOC (%)	80.00
Calculated energy level left in battery (kWh)	46.08

	Results		
User no.	Energy consumption 00:00 - 18:00 by each user (kWh)	Energy left for each load to use after 18:00	
		(kWh)	(%)
1	14.00	14.66	31.82
2	10.50	16.76	36.36
3	14.00	14.66	31.82
Total	38.50	46.08	100

Table 7.4 shows a summary of the results, indicating the SOC and energy statuses. Percentages of charge division also show the energy amounts that were divided among the individual users.

8. CONCLUSIONS AND RECOMMENDATIONS

8.1. Conclusions

An energy reserve share concept was introduced by the development of a control algorithm on the Matlab software platform. The model has been developed in such a way that the Matlab simulation user can interact with the model via the model parameters. The slower real-time speed of model simulation also allows the user to see how parameters change while control processing is performed.

Four scenarios were set up to test if the developed algorithm is functional and to verify that mathematically the charge share formula executes grid control correctly. The purpose of the algorithm is to facilitate the allocation of electric energy among the grid users at 18:00, to allow use of energy up to 24:00. Battery SOC and user energy consumption during the day are the determining factors for apportioning the available stored energy among the users.

Scenario A showed a result where equal energy from the remaining state-of-charge was shared between the grid users. Scenarios B and C were setup with variable load changes over a 24-hour period. In both Scenarios B and C the allocation of stored energy was done in accordance with the users energy consumption between 00:00 and 18:00. Users with a high amount of energy consumption before 18:00, were allocated a smaller portion of energy from the available stored energy, while users of a low amount of energy (small power users) were allocated a larger portion of energy from the remaining available energy stored.

Islanded MAS grids are affected by a limited energy storage capacity. By using this concept for allocating stored energy for rural-electric applications, electric energy can be divided among multiple users in accordance with their daily use and the remaining amount of available energy stored in the battery.

8.2. Future research

In addition to this agent-based algorithm developed and tested in this work, a token system can be developed where users can sell the electric energy allocated to them from the stored energy, to other users.

Another option is to integrate switches inside the homes. These devices act as user inputs to the charge share control management system. When a house is unoccupied for a long duration, the user should be able to disconnect his house from the grid. The charge share decisional formula would be adjusted accordingly. More energy will then be available for sharing among the remaining users. The PV panels can still be active to supply the microgrid

of energy if some of these are located on the roof of the house of a user who has been disconnected. All the generation units should be active at all possible opportunities so as to give maximum efficiency to the charge agents on the grid.

A critical load scheme can be integrated into this grid. Lighting control can be added to the model. Whenever all the users have depleted their charge capacity, then a separate critical load area can be designed to control and manage critical loads from a certain percentage of remaining battery capacity that has been reserved. Lighting control is critical to provide sufficient light to the community during night hours.

8.3. Publication emanating from the thesis

The following publication was produced during the course of this research investigation:

Vosloo A and Raji AK, “Intelligent Central Energy Management System for Remote Community Microgrid”. Domestic Use Energy Conference, Cape Town, South Africa, 31 March–1 April, 2015. pp. 137–140.

REFERENCES

Andreadis, G. Klazoglou, P. Noitaki, K. Bouzakis, K. D. (2013) Classification and Review of Multi-Agent Systems in the Manufacturing Section. *24th DAAAM International Symposium on Intelligent Manufacturing and Automation.* Procedia Engineering 69. pp. 282–290.

Andreadis, G. Bouzakis, K. D. Klazoglou, P. Niwtaki, K. (2014) Review of Agent – Based Systems in the Manufacturing Section. *Universal Journal of Mechanical Engineering*. 2 (2). pp. 55–59.

Back to the source. (2015). Cape Solar Power. [Online] Available from: http://www.backtothesource.co.za/index.php/cape-solar-power/. [Accessed: 20 January 2015]

Boynuegri, A. R., Yagcitekin, B., Baysal, M., Karakas, A. & Uzunoglu, M. (2013). *Energy Management Algorithm for Smart Home with Renewable Energy Sources. In Power Engineering, Energy and Electrical Drives (POWERENG), 2013 Fourth International Conference.* 13–17 May 2013. pp. 1753–1758.

Btekenergy (2015).Solar energy FAQ. How do solar cells generate electricity [Online] Available from: http://www.btekenergy.com/documents/88.html [Accessed: 17 January 2015]

Bullis, K. (2012) Sun Edition Turns to Big New Markets for Solar Power. *MIT Technology Review.* [Online] 8 June. Available from: http://www.technologyreview.com/photogallery/428100/sunedison-turns-to-big-new-markets-for-solar-power/?nlid=nlenrg&nld=2012-06-11. [Accessed: 9 August 2014]

Business Times. (2014) “It doesn’t pay to connect Africa’s poor to the grid”. [Online] Available: http://www.bdlive.co.za/businesstimes/2014/05/04/the-chatter-it-doesn-t-pay-to-connect-africa-s-poor-to-the-grid.

Chan, J. (2012) Update: Tokelau islands powered by 100% solar. *PV TECH.* [Online] Available from: http://www.pv-tech.org/news/tokelau_islands_powered_by_100_solar [Accessed: 5th August 2014]

Chang, J. Jai, S (2009) Modeling and application of wind-solar energy hybrid power generation system based on Multi-Agent Technology. In *Proceedings of the eighth International Conference on Machine Learning and Cybernetics*. Baoding, 12–15 July 2009. pp. 1754–1758.

Chaouachi, A., Kamel, R. M., Andoulsi, R. & Nagasaka, K. (2013). Multiobjective Intelligent Energy Management for a Microgrid*. Industrial Electronics, IEEE Transactions* [Online] Volume: 60, Issue: 4. pp. 1688–1699. Available from: http://ieeexplore.ieee.org.ezproxy.cput.ac.za/stamp/stamp.jsp?tp=&arnumber=6157610 [Accessed: 06 May 2014]

Cleantechnica. (2014) New solar cell efficiency record set at 46%. [Online] Available from: http://cleantechnica.com/2014/12/03/new-solar-cell-efficiency-record-set-46/ [Accessed: 17 January 2015]

Fitzpatrick, E. (2014). India village claims a first - 100 % solar storage microgrid. *Reneweconomy.* [Online] 21 July. Available from: http://www.reneweconomy.com.au/2014/india-village-claims-a-first-100-solar-storage-micro-grid-81573. [Accessed: 9 August 2014]

Greenpeace. (2014). Dharnai Live Microgrid Media Manual. [Online] Available from: http://www.greenpeace.org/india/en/publications/Dharnai-Live-Microgrid-Media-Manual-/. [Accessed: 19 May 2015]

GeoSun Africa. (2014) Updated satellite maps of South Africa's solar resource now available. [Online] Available from - http://geosun.co.za/.[Accessed: 17 January 2015]

Hajimohamadi, N. Bevrani, H. (2013) Load shedding in microgrids. In - Electrical Engineering (ICEE), 2013 21st Iranian Conference. Mashhad. 14–16 May 2013. pp. 1–6.

Hernandez, F. Canesin, C. A. Zamora, R. Martina, F. Srivastava, A. K. (2013) Energy Management and Control for Islanded Microgrid Using Multi – Agents. In *North American Power Symposium (NAPS)* .Manhattan, KS. 22–24 September. pp. 1–6.

Jian, Z., Qian, A., Chuanwen, J., Xingang, W., Zhanghua, Z. & Chenghong, G. (2009). The application of Multi Agent System in Microgrid coordination control. *Sustainable power generation and supply*, *Supergen*. pp. 1–6.

Jimeno, J. Anduaga, J. Oyarzabal, J. Gil de Muro, A. (2010) Architecture of a microgrid energy managements system. In - *European Transaction on Electrical Power.* Spain. 26 April. pp. 1142–1158.

Kennedy, J. Ciufo, A. Agalgaonkar, A. (2012) intelligent load management in Microgrids. In - Power and Energy Society General Meeting, IEEESan Diego. July 22–26 2012. pp. 1–8.

Lantero, A. (2013). *The War of the Currents: AC vs. DC Power.* Washington DC, Energy. Gov.

Li, W., Mou, X., Zhou, Y. & Marnay, C. (2012). On Voltage Standards for DC Home Microgrids Energized by Distributed Sources. In - *7th International Power Electronics and Motion Control Conference - ECCE Asia.* June 2–5, 2012, Harbin, China. IEEE. pp. 2282–2286.

Logenthiran, T., Srinivasan, D., Khambadkone, A. M. & Aung, H. N. (2010).Multi-Agent System (MAS) for Short-Term Generation Scheduling of a Microgrid.*IEEE ICSET Sri Lanka.*[Online] pp.1–6. Available from: http://ieeexplore.ieee.org.ezproxy.cput.ac.za/stamp/stamp.jsp?tp=&arnumber=5684943 [Accessed: 03 May 2014]

Manickavasagam, K., Nithya, M., Priya, K., Shruthi, J., Krishnan, S., Misra, S.& Manikandan, S. (2011). Control of distributed generator and smart grid multi-agent system. In - *Electrical Energy Systems (ICEES)*, 1st International Conference, pp. 212–217.

Meiqin, M., Wei D. &Chang, L. (2011).Multi-agent based simulation for Microgrid energy management. In *8th International conference on Power Electronics* and ECCE*.* Asia. May 30 2011–June 3 2011. IEEE Conference Publications. pp. 1219–1223.

Michaelson, D. Mahmood, H. Jiang, J. (2013) A predictive energy management strategy with pre-emptive load shedding for an islanded PV-battery microgrid. In: Industrial Electronics Society, IECON 2013 - 39th Annual Conference of the IEEE. Vienna. 10–13 November 2013. pp. 1501–1506.

Nehrir, M, H., Wang, C., Strunz, K., Aki, H., Ramakumar, R., Bing, J., Maio, Z. & Salameh, Z. (2011).Review of Hybrid Renewable / Alternative Energy Systems for Electric Power Generation: Configurations, Control, and Applications in - *IEEE Transactions on sustainable energy*. [Online] Vol. 2. Issue 4. pp. 392–403.

Nejabatkhah, F. Wei Li, Y. (2014). Overview of Power Management Strategies of Hybrid AC/DC Microgrid. In - Power Electronics, IEEE Transactions, Issue 99. 22 December 2014. pp. 1.

Northern Arizona wind and sun. (2015) All about maximum power point tracking (mppt) solar charge controllers. [Online] Available from - http: //www.solar-electric.com/mppt-solar-charge-controllers.html/. [Accessed: 17 January 2015]

Palma-Behnke, R., Reyes, L. & Jiménez - Estévez, G. (2012) Smart grid solutions for rural areas. *Power and Energy Society General Meeting, 2012 IEEE.* 22–26 July 2012. pp. 1–6.

Phys.Org, Oct 04, 2013, bringing sustainable electricity to rural African communities. [Online] http://phys.org/news/2013-10-sustainable-electricity-rural-african.html. [Accessed: 15 May 2014]

P. Mcgroarthy. (2012) "Power to More People", *The journal report: Innovations in energy*. Available: http://online.wsj.com/articles/

Polycarpou, L. (2013). The Microgrid Solution [Online] 15 May 2013. Available from http://blogs.ei.columbia.edu/2013/05/15/the-microgrid-solution/ [Accessed: 4 June 2014]

Potty, K. A., Keny, P. & Nagarajan, C. (2013).An Intelligent Microgrid with Distributed Generation. IEEE *Innovative Smart Grid Technologies - ISGT Asia.* [Online].pp. 1–5. Available from: http://ieeexplore.ieee.org.ezproxy.cput.ac.za/stamp/stamp.jsp?tp=&arnumber=6698755. [Accessed: 03 May 2014]

PowerSmart. (2012). Available from http://powersmartsolar.co.nz/our_projects/id/185 [Accessed: 18 May 2015]

Qin, Q. Chen, Z. Wang, Z. (2012). Overview of micro-grid energy management system research status. In *Power Engineering and Automation Conference (PEAM), IEEE*. Wuhan. 18–20 September. pp. 1–4.

Radziszewska. & Nahorski, Z. (2013). Simulation of energy consumption in a microgrid for demand side management by scheduling. In *Computer Science and Information Systems (FedCSIS).* 8–11 Sept. 2013. pp. 679–682.

Ramesh, R., Karan, K.,Vineeth,V.& Dhiwaakar, P. (2013).Implementation of Arduino-based Multi-Agent System for Rural Indian Microgrids.In – IEEE PES *Innovative Smart Grid Technologies (ISGT)*. Chennai, India

SABS, 2012. SANS 10142-1:2009 (ed. 1.7) THE WIRING OF PREMISES - PART 1: LOW-VOLTAGE INSTALLATIONS. South Africa: SABS STANDARDS DIVISION.

Salmi, T. Bouzquenda, M. Gastli, A. Masmoudi, A. (2012). Matlab / Simulink based modelling of solar photovoltaic cell. International Journal of renewable energy research. Vol. 2, No. 2, 2012. pp. 213–218.

Schnitzer, D., Lounsbury, D., Carvallo, J., Deshmukh, R., Apt, J. & Kammen, D. (2014). Microgrids for Rural Electrification. *IEEE Smart Grid*. [Online] Available from http://smartgrid.ieee.org/april-2014/1071-microgrids-for-rural-electrification [Accessed: 15 May 2014]

Solare, New energy technology (2015).High efficient poly PV solar panel 350 Watt 48 V for home system. [Online] Available from - http://solare.en.alibaba.com/product/542433162-220834565/High_efficient_poly_PV_solar_panel_350Watt_48V_for_home_system.html. [Accessed: 20 January 2015]

Solar direct (2015). Solar electric system sizing. [Online] Available from http://solardirect.com/pv/systems/gts/gts-sizing-array.html [Accessed: 20 January 2015]

Solarenergyexplorer (2015).Maximum Power Point Tracking. [Online] Available from: http://www.solarenergyexplorer.com/maximum-power-point-tracking.html [Accessed: 17 January 2015]

Stluka, P., Godbole, D. & Samad, T. (2011).Energy Management for Buildings and Microgrids. In - 50th IEEE Conference on Decision and Control and European Control Conference (CDC-ECC). Orlando, FL, USA, December 12–15, 2011.

Syed, I & Weidong, X. (2012). Modelling and control of DAB applied in a PV based DC microgrid. In - *International Conference on Power Electronics, Drives and Energy Systems.* Bengaluru, India*.* December 16–19*.* pp. 1–6.

Xinhua, L. Xutang, Z. Wenjian, L. (2007) Integration of CAPP and CAFD based agent technology. In - *International Conference on Mechatronics*. Kumamoto Japan. 8–10 May 2007.

Yen-Haw, C., Yen-Hong, C. & Ming-Che, H. (2011).Optimal Energy Management of Microgrid Systems in Taiwan.In: IEEE PES *Innovative Smart Grid Technologies (ISGT)*. [Online]. pp. 1–9. Available from: http://ieeexplore.ieee.org.ezproxy.cput.ac.za/xpl/articleDetails.jsp?tp=&arnumber=5759149&queryText%3Denergy+management+microgrid+taiwan. [Accessed: 12 May 2014]

Zamostny, D. (2013). Solar history: Alexandre Edmond Becquerellar [Online] 2 December 2013. Available from http://www.solarenergyworld.com/2011/06/17/solar-history-alexandre-edmond-becquerel/ [Accessed: 4 June 2014]